

AD-A186 720 REPORT DOCUMENTATION PAGE

2a. SECURITY CLASSIFICATION AUTHORITY		1b. RESTRICTIVE MARKINGS	
2b. DECLASSIFICATION / DOWNGRADING SCHEDULE		3. DISTRIBUTION / AVAILABILITY OF REPORT Approved for public release, distribution unlimited	
4. PERFORMING ORGANIZATION REPORT NUMBER(S)		5. MONITORING ORGANIZATION REPORT NUMBER(S) AFOSR-TR- 87-1373	
6a. NAME OF PERFORMING ORGANIZATION	6b. OFFICE SYMBOL <i>(if applicable)</i>	7a. NAME OF MONITORING ORGANIZATION AFOSR	
6c. ADDRESS (City, State, and ZIP Code) Brandeis University Waltham, MA 02254		7b. ADDRESS (City, State, and ZIP Code) Building 410 Bolling AFB DC 20332-6448	
8a. NAME OF FUNDING / SPONSORING ORGANIZATION AFOSR	8b. OFFICE SYMBOL <i>(if applicable)</i> NP	9. PROCUREMENT INSTRUMENT IDENTIFICATION NUMBER AFOSR-84-0014	
8c. ADDRESS (City, State, and ZIP Code) Building 410 Bolling AFB, DC 20332-6448		10. SOURCE OF FUNDING NUMBERS	
		PROGRAM ELEMENT NO 61102F	PROJECT NO. 2301
		TASK NO. A8	WORK UNIT ACCESSION NO
11. TITLE (include Security Classification) "SLIDING CHARGE DENSITY WAVES AND RELATED PROBLEMS" (U)			
12. PERSONAL AUTHOR(S)			
13a. TYPE OF REPORT FINAL	13b. TIME COVERED FROM 83/11/01 TO 87/03/31	14. DATE OF REPORT (Year, Month, Day)	15. PAGE COUNT 39
16. SUPPLEMENTARY NOTATION			
17. COSATI CODES		18. SUBJECT TERMS (Continue on reverse if necessary and identify by block number)	
FIELD	GROUP	SUB-GROUP	Sliding Density Waves, Sliding Potential
19. ABSTRACT (Continue on reverse if necessary and identify by block number)			
<p>From the publications (in many cases from the Figures) it is seen that incommensurate chains give a surprisingly good account of the following dozen measurements: both components of complex conductivities as functions of field and frequency, in both metallic and semiconducting CDW materials; dc characteristics; scaling of ac and dc conductivities; elastic properties - Young's Modules and Q-factor as functions of voltage; bulk oscillations; and both amplitude and phase of both the second and third order mixing properties. In addition, incommensurate chains have been seen to exhibit complete mode locking over the entire range of dc fields and external frequencies. (These results resolve a dispute between the Illinois and the AT&T Bell Laboratories groups. The manuscript is being prepared for Physical Review Letters and the abstract is included in section III.)</p>			
20. DISTRIBUTION / AVAILABILITY OF ABSTRACT <input checked="" type="checkbox"/> UNCLASSIFIED/UNLIMITED <input checked="" type="checkbox"/> SAME AS RPT <input checked="" type="checkbox"/> DTIC USERS		21. ABSTRACT SECURITY CLASSIFICATION UNCLASSIFIED	
22a. NAME OF RESPONSIBLE INDIVIDUAL DR. ROBERT J. BARKER		22b. TELEPHONE (Include Area Code) (202)767-5011	22c. OFFICE SYMBOL NP

DTIC
OCT 25 1987
CDE

1 NOV 83 to 31 MAR 87

FINAL TECHNICAL REPORT

AFOSR-TR. 87-1373

Re: Grant No. AFOSR-84-0014

Brandeis University, Waltham, MA 02254

Principal Investigator: L. Sneddon

Contents:

- I. Goals of the Research
- II. Theory vs. Experiment
- III. Publications
- IV. Collective Nonlinearity in Solids
- V. The Threshold: a Surviving Challenge

AFOSR-TR. 87-1373	
Final Report	<input checked="" type="checkbox"/>
Technical Report	<input type="checkbox"/>
Summary Report	<input type="checkbox"/>
Date: 11/1/83	
Author: L. Sneddon	
Sponsor: AFOSR	
Project: Nonlinear Dynamics	
Contract: AFOSR-84-0014	
Work Unit: 1	
Page: A-1	



I. Goals of the Research

This Grant aimed at an understanding of the strongly nonlinear electrical properties of charge density wave (CDW) conductors.

Some progress had been made, in understanding weakly nonlinear properties, with models which retained the spatial randomness of the pinning potential (due to crystal inhomogeneities). The complexity of a random potential (when combined with the dynamic, many-body and nonlinear nature of the problem) meant however that progress into the strongly nonlinear regime was extremely slow, despite the attentions of numerous researchers. The PI adopted what was at the time a somewhat unfashionable approach. It was decided to see whether the randomness in the pinning potential might not in fact be an unnecessary complication. It was decided to attempt to solve for the dynamical properties of incommensurate chains. These have a periodic rather than a random pinning potential, but they retain the collective, or many-body, aspect as well as the nonlinearity of sliding CDW's. Once their dynamic properties are solved we must compare with experiment to see whether these models really contain the essence of CDW conduction.

The results are summarized in the next section (II). A more complete account of the progress under the grant is contained in

the publications (Section III), with some ongoing work described in the final section (V). In section IV, I outline a new perspective that has emerged from the results of all these projects taken as a whole.

II. Theory vs. Experiment

From the publications (in many cases from the Figures) it is seen that incommensurate chains give a surprisingly good account of the following dozen measurements: both components of complex ac conductivities as functions of field and frequency, in both metallic and semiconducting CDW materials; dc characteristics; scaling of ac and dc conductivities; elastic properties - Young's Modulus and Q-factor as functions of voltage; bulk oscillations; and both amplitude and phase of both the second and third order mixing properties. In addition, incommensurate chains have been seen to exhibit complete mode locking over the entire range of dc fields and external frequencies. (These results resolve a dispute between the Illinois and the AT&T Bell Laboratories groups. The manuscript is being prepared for Physical Review Letters and the abstract is included in section III.)

III. Publications

1. Sliding Dynamics of the Incommensurate Chain
Physical Review Letters, 52, 65 (1984).
2. Dynamics of Incommensurate Structures: An Exact Solution
Physical Review (Rapid Communications), B30, 2974 (1984).
3. Electromechanical Properties of Charge Density Wave Conductors
Physical Review Letters, 56, 1194 (1986).
4. Oscillatory Instability in the Dynamics of Incommensurate Structures
Physical Review Letters, 58, 1903 (1987).
5. Mixing in Charge Density Wave Conductors
Physical Review (Rapid Communications) B35, 7745 (1987).
6. Mode Locking in Charge Density Waves: a Classical Theory
to be submitted to Physical Review Letters.

PUBLICATION 1.

Sliding Dynamics of the Incommensurate Chain

Leigh Sneddon

Martin Fisher School of Physics, Brandeis University, Waltham, Massachusetts 02254

(Received 8 July 1983)

The dc dynamics of the sliding incommensurate chain is reduced to a purely static problem. The sliding system is described by a static hull function which becomes singular, above the critical pinning strength, as the velocity approaches zero. Both ac and dc sliding dynamics are determined numerically for the cases of weak and strong pinning and short- and long-range interactions. Excellent agreement is obtained with experiments on sliding charge-density waves near threshold, both in NbSe₃ and in TaS₃.

PACS numbers: 72.15.Nj, 72.15.Eb, 72.20.Ht

Incommensurate structures, such as charge-density waves (CDW's) and adsorbed monolayers, are now familiar in solid-state physics.¹ The discovery² of electrical conduction due to sliding CDW's raised a wide range of questions concerning the dynamics of sliding incommensurate structures. This article reports progress in the analytic study of such dynamics and in the understanding of related experimental results.

The incommensurate system studied here is a simple extension of the model of Frenkel and Kontorova,³ and the dimensionless equations of motion can be written

$$\begin{aligned} \dot{u}_j + \sum_p K_p (2u_j - u_{j-p} - u_{j+p}) \\ = f + P \cos H(j + u_j), \end{aligned} \quad (1)$$

where $j = 1, 2, \dots, N$, P is the strength of the pinning force, and $2\pi/H$ its wavelength. The case of

$$v = f - PF_0\{w_m\}, \quad (3a)$$

$$\dot{w}_\mu = -(2i[1 - \sum_p K_p \cos \mu H p] - i_\mu H v) w_\mu + PF_\mu\{w_m\} \quad (3b)$$

for $1 \leq \mu \leq N/2$, where

$$F_\mu\{w_m\} \equiv N^{-1} \sum_{j=1}^N e^{-i\mu H j} \cos H(j - 2 \sum_{1 \leq m < N/2} a_m \cos(mHj + \alpha_m)), \quad (3c)$$

independent of w_ν .

For constant v , static solutions, with $\dot{w}_\mu = 0$ for $\mu \geq 1$, were found. A finite number, μ_{max} , of the w_μ were retained and the corresponding coupled equations (3b) were solved numerically, treating the retained w_μ to all orders. The couplings in (3c) were computed with N large enough that increasing it had no significant effect. These solutions were tested in two ways. Firstly, the dc characteristic was calculated. With weak pinning, clear convergence, with increasing μ_{max} , to a linear response at $v = 0$ was found, with no threshold. For strong pinning the emergence of a threshold singularity, with increasing μ_{max} ,

$N \rightarrow \infty$ and $H/2\pi$ equal to an irrational, ρ , was studied by considering $H/2\pi = M_N/N$, where M_N is an integer, having no common factor with N , and $M_N/N \rightarrow \rho$ as $N \rightarrow \infty$.

Equation (1) was Fourier transformed to replace the u_j 's by phase-shifted Fourier components $w_m = a_m \exp(i\alpha_m)$:

$$w_m = \exp(-imHw_0) N^{-1} \sum_{j=1}^N \exp(-imHj) u_j \quad (2)$$

for $m = 0, 1, 2, \dots, N-1$. Using Bessel functions to expand the cosine in (1) gives terms with an explicit N dependence. As $N \rightarrow \infty$ for a bulk velocity $v > 0$, these terms can be shown to vanish to every finite order of perturbation in P and oscillate at arbitrarily high frequencies about zero. To treat the limit $N \rightarrow \infty$, only those terms with no explicit N dependence were retained.

This gives

$$v = f - PF_0\{w_m\}, \quad (3a)$$

$$\dot{w}_\mu = -(2i[1 - \sum_p K_p \cos \mu H p] - i_\mu H v) w_\mu + PF_\mu\{w_m\} \quad (3b)$$

for $1 \leq \mu \leq N/2$, where

$$F_\mu\{w_m\} \equiv N^{-1} \sum_{j=1}^N e^{-i\mu H j} \cos H(j - 2 \sum_{1 \leq m < N/2} a_m \cos(mHj + \alpha_m)), \quad (3c)$$

independent of w_ν .

For constant v , static solutions, with $\dot{w}_\mu = 0$ for $\mu \geq 1$, were found. A finite number, μ_{max} , of the w_μ were retained and the corresponding coupled equations (3b) were solved numerically, treating the retained w_μ to all orders. The couplings in (3c) were computed with N large enough that increasing it had no significant effect. These solutions were tested in two ways. Firstly, the dc characteristic was calculated. With weak pinning, clear convergence, with increasing μ_{max} , to a linear response at $v = 0$ was found, with no threshold. For strong pinning the emergence of a threshold singularity, with increasing μ_{max} ,

was clearly indicated. The results thus agree with present knowledge⁴ at low velocities and are also correct to all orders in perturbation theory at moderate and high velocities. Secondly, the solutions were tested for stability to small perturbations and were found to be dynamically stable.

Since these solutions are static, exploiting translational invariance has transformed the dc sliding dynamics of the infinite incommensurate chain to a purely static problem.

From (2), the Fourier components, w_m , of the distortions then have a simple time dependence:

$y_m = \text{const} \times e^{imHt}$. (A corresponding result for excitations about the $v=0$ limit was obtained by Novaco.³) Further, there is a static hull function describing dc sliding solutions with $v > 0$. That is, $u_j - vt$ is a function of a single variable:

$$u_j - vt = g_v(j - vt), \quad (4)$$

where the periodic function g_v is given by

$$g_v(x) = 2 \sum_{1 \leq m < N/2} a_m \cos(mHx + \alpha_m). \quad (5)$$

Much attention has been given^{1,6} to the way, at $f=v=0$, g_v changes from being analytic, for weak pinning, to singular, for strong pinning. The present studies showed the amplitudes a_m decaying exponentially with m when $v > 0$, even with strong pinning. The function g_v is then analytic for $v > 0$. Thus for strong pinning a breaking-of-analyticity transition occurs in the new hull function, as the velocity approaches zero at threshold. The complicated time dependence of the $u_j(t)$ near threshold is expressed, by (4), completely in terms of the emergence of singularities in this new hull function.

Linear ac response, in the presence of a dc field, has been studied experimentally⁷ in the CDW systems NbSe₃ and TaS₃. At fields a few times threshold low-order perturbation theory⁸ is not useful; but this region is the most commonly studied experimentally because the nonlinear effects are larger than in the high-field region, and sample heating is not a problem. The pres-

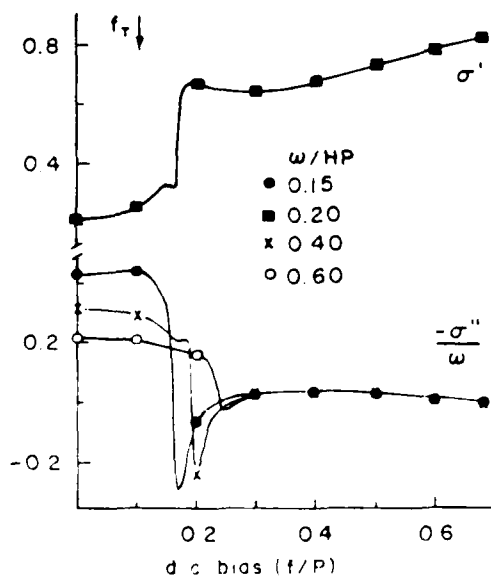


FIG. 1. ac response of sixfold-coordination incommensurate chain, showing interference features.

ent techniques were therefore used to determine the ac response of the sliding incommensurate chain near threshold. Having reduced the dc dynamics to a static problem is very useful. The ac response of a time-dependent solution is much more difficult to obtain than that of a static solution, for which the ac response, like the dc characteristics, can be determined without numerical integration.

The CDW's in NbSe₃ and TaS₃ are three-dimensionally coherent.⁹ One effect of higher dimensionality is to increase the coordination of the system. To mimic this increased coordination crudely, a sixfold-coordinated chain was considered with $K_1 = K_2 = K_3 = \frac{1}{3}$; $K_p = 0$, $p > 3$.

By considering in (3) a small perturbation about a static dc solution, the ac response, $\sigma(\omega) = \sigma' + i\sigma''$ was determined, for¹⁰ $\rho = (5^{1/2} + 1)/2$ and $HP = 3.0$. The results (with $\mu_{max} = 15$) for σ' and the dielectric response $-\sigma''/\omega$ are shown in Fig. 1. The basic features in Figs. 1, 3, and 5 are preserved with increasing μ_{max} . The threshold force was estimated from the dc results.

Figure 2 shows experimental results⁷ for $\text{Re}\sigma_{tot}(\omega)$ and $\epsilon(\omega)$ of the sliding charge-density wave in NbSe₃. Figure 1 is seen to account well for the voltage and frequency dependence of both

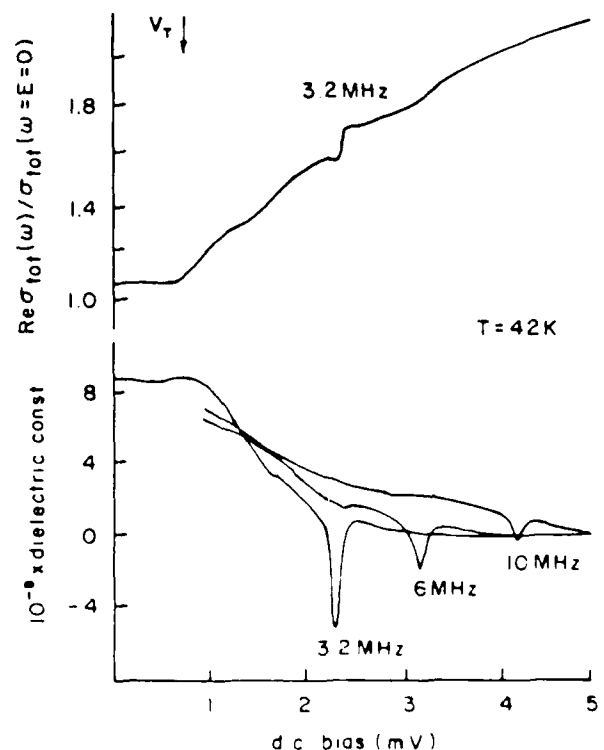


FIG. 2. ac response (Ref. 7) of NbSe₃.

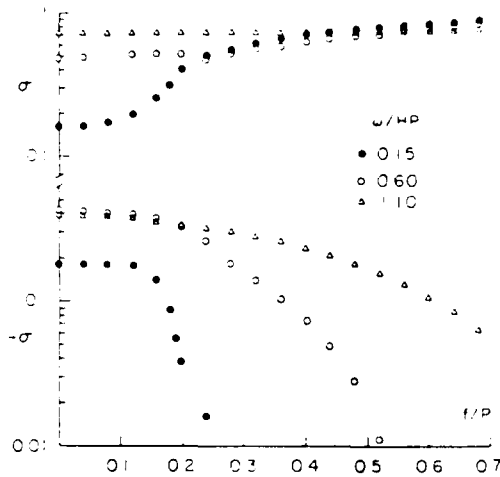


FIG. 3. ac response of incommensurate chain with infinite-range interactions; c.f. Fig. 4 and text.

components of the ac response. This may not have been expected since CDW dynamics are dominated by randomly positioned defects¹¹ while the chain is in a periodic potential.

In experiments⁷ performed on TaS₃ at 130 K, the sharp interference features seen⁷ with NbSe₃ (Figs. 1 and 2) were not observed. TaS₃ becomes a semiconductor¹² below the CDW transition, while NbSe₃ is metallic.² At 130 K the conductivity of TaS₃ has fallen two orders of magnitude from its value at the transition. As discussed earlier,¹³ this reduces the screening capacity of the normal electrons and can allow long-range Coulomb interactions of the CDW with itself.

The sliding dynamics of Eq. (1) with long-range interactions, $K_p = 2/N$ for all p , was therefore determined. The results (with $\mu_{max} = 20$) are shown in Fig. 3, and can be compared with the experimental results in Fig. 4. Not only does including long-range interactions account for the absence of interference features, but the properties of the incommensurate chain are seen to match those of TaS₃ extremely well. The *difference* between the ac properties of NbSe₃ and TaS₃ can now be understood for the first time as being due to the presence in TaS₃, as suggested earlier,¹³ of long-range Coulomb interactions of the CDW with itself.

The ac response was also determined with $f = 0$, and compared to the dc conductivity σ_{dc} . The results (with $\mu_{max} = 20$) are shown in Fig. 5 for long-range interactions. Similar results were obtained for the sixfold-coordinated chain. The experimentally observed^{14,15} scaling, of field- and frequency-dependent conductivities,

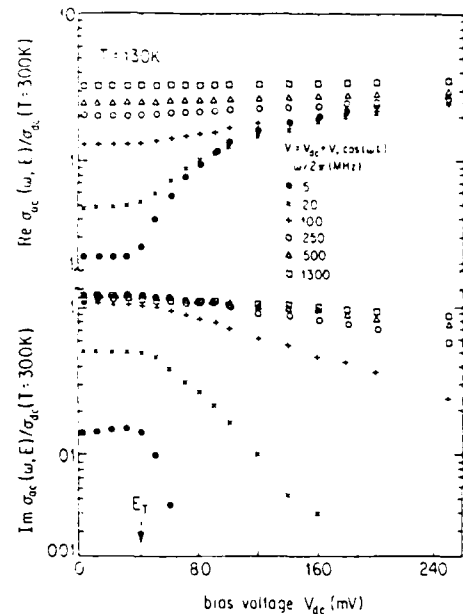


FIG. 4. ac response (Ref. 7) of TaS₃.

is thus exhibited by this *classical* model, and can no longer be regarded¹⁵ as evidence for a quantum mechanical theory of CDW conductivity.

Although these calculations do not probe asymptotic low-frequency threshold properties it is interesting to speculate that the detailed form of the potential becomes less important as one approaches threshold. In any case, the comparison of theory with experiment seen in Figs. 1-5 shows that, in fields comparable to threshold, the incommensurate chain gives a much better picture of CDW dynamics than might have been suspected.

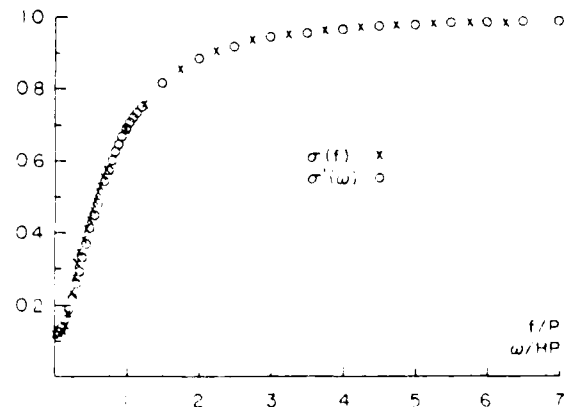


FIG. 5. Scaling of field-dependent (crosses) and frequency-dependent (circles) conductivities in the classical chain.

The author enjoyed discussions with S. Copper-smith, M. Cross, D. Fisher, E. Gross, and P. Littlewood, and thanks A. Zettl and G. Grüner for permission to reproduce experimental results prior to publication.

¹P. Bak, Rep. Prog. Phys. 45, 587 (1982).

²P. Monceau *et al.*, Phys. Rev. Lett. 37, 602 (1976).

³Y. I. Frenkel and T. Kontorova, Zh. Eksp. Teor. Fiz. 5, 1340 (1938); F. C. Frank and J. H. van der Merwe, Proc. Roy. Soc. London, Ser. A 198, 205 (1949).

⁴M. Peyrard and S. Aubry, J. Phys. C 16, 1593 (1983).

⁵A. D. Novaco, Phys. Rev. B 22, 1645 (1980).

⁶S. J. Shenker and L. P. Kadanoff, J. Stat. Phys. 27, 631 (1982).

⁷A. Zettl and G. Grüner, to be published.

⁸L. Sneddon, M. C. Cross, and D. S. Fisher, Phys. Rev. Lett. 49, 292 (1982).

⁹R. M. Fleming *et al.*, Phys. Rev. B 18, 5560 (1978); K. Tsutsumi *et al.*, J. Phys. Soc. Jpn. 44, 1735 (1978).

¹⁰All the results presented here hold for any $H=2-pz \pmod{2\pi}$.

¹¹N. P. Ong *et al.*, Phys. Rev. Lett. 42, 811 (1979).

¹²T. Takoshima *et al.*, Solid State Commun. 35, 911 (1980).

¹³L. Sneddon, to be published.

¹⁴G. Grüner, Mol. Cryst. Liq. Cryst. 81, 17 (1982);

A. Zettl *et al.*, Phys. Rev. B 26, 5773 (1982); G. Grüner *et al.*, Phys. Rev. B 24, 7247 (1981).

¹⁵J. Bardeen, Phys. Rev. Lett. 45, 1978 (1980);

A. Zettl and G. Grüner, Phys. Rev. B 25, 2081 (1982);

J. Bardeen, Mol. Cryst. Liq. Cryst. 81, 1 (1982);

J. H. Miller, Jr., J. Richard, J. R. Tucker, and

J. Bardeen, Phys. Rev. Lett. 51, 1592 (1983).

PUBLICATION 2.

Dynamics of incommensurate structures: An exact solution

Leigh Sneddon

The Martin Fisher School of Physics, Brandeis University,
Waltham, Massachusetts 02254

(Received 13 March 1984)

A simple exact solution of the incommensurate chain with infinite-range interactions is obtained with the use of both analytic and graphical techniques. The ground states and all metastable states are identified. Results are derived for the depinning transition, the sliding threshold, and the excitation spectrum as a function of pinning strength and applied field. The ac response is also obtained and has a low-frequency singularity at threshold, but the dielectric constant is bounded, as seen in charge-density-wave experiments.

Incommensurate structures, such as charge-density waves (CDW's) and adsorbed monolayers, are well known in solid-state physics.¹ The incommensurate harmonic chain has recently been seen² to provide a useful model of CDW conductivity and long-range interactions have been seen^{2,3} to be important in semiconductor CDW systems, e.g., TaS₃.

If every particle in a chain interacts equally with every other, the equation of motion can be written

$$\frac{dU_j}{dt} = f(t) + P \sin(Hj + U_j) + \langle U \rangle - U_j \quad (1)$$

Here $j = 1, 2, \dots$

$$\langle U \rangle = \lim_{N \rightarrow \infty} N^{-1} \sum_{j=1}^N U_j$$

P is the strength of the pinning force, and $2\pi/H$ its wavelength, an irrational. Fisher⁴ has studied the related problem where P is replaced by a randomly distributed variable. The purposes of this Rapid Communication are to provide a considerably simpler exact solution of the incommensurate case (fixed P) and to derive a number of new exact results.

Solutions to (1) can be written

$$U_j(t) = \alpha(t) + g(Hj + \alpha(t); t) \quad (2)$$

where⁵ $g(x + 2\pi; t) = g(x, t)$, and

$$f(t) = -(2\pi)^{-1} \int_{-\pi}^{\pi} dx g(x; t) \quad (3)$$

Substituting (2) in (1) and using the identity

$$\lim_{N \rightarrow \infty} N^{-1} \sum_{j=1}^N F(\gamma_j) = \int_0^1 F(x) dx$$

for γ irrational and $F(x+1) = F(x)$ gives

$$\alpha(t) \left(1 + \frac{\partial g}{\partial x} \right) + \frac{\partial g}{\partial t} = P \sin(x + g) - g \quad (4)$$

where, for bulk velocity $v(t) \equiv d\langle U \rangle/dt$, α satisfies

$$v(t) = \alpha(t) - t(t) \quad (5)$$

Thus, the form (2) yields an equation of motion which depends on $v \equiv d\langle U \rangle/dt$, but not on $\langle U \rangle$, exhibiting the translational invariance of the incommensurate system.⁶

The transient and hysteretic properties of (1) are currently under investigation. The rest of this article will consider

constant f , in which case $\dot{\alpha}$ and v are constant, and one can search for solutions⁷ with $\partial g/\partial t = 0$. Equations (2), (4), and (5) then simplify⁸ to

$$U_j(t) = \alpha + g(Hj + \alpha) \quad (6)$$

$$v(1 + g') = P \sin(x + g) - g \quad (7)$$

When $v = 0$, (6) is a simple transcendental equation which can be solved graphically. For $P < 1$ there is a unique solution [Fig. 1(a)]. It is continuous and odd so that, using (3), when $v = 0$, $f = 0$, and there is no sliding threshold. For $P > 1$ there are multiple, discontinuous solutions, g , many with nonzero means [Figs. 1(b) and 1(c)]. The threshold force is clearly

$$f_T = \max_{\alpha} -(2\pi)^{-1} \int_{-\pi}^{\pi} g(x) dx \quad (8)$$

Thus the critical value of P defining the depinning transition

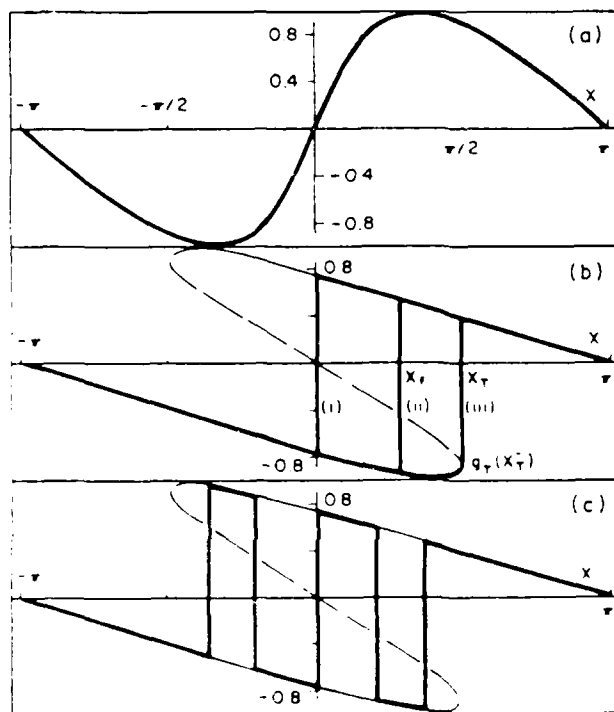


FIG. 1. Stationary states $g(x)$: (a) $P=0.5$; (b) $P=3$, ground states for $t=0$, (i) $0 < t < t_p$, (ii) $t = t_p$, $v < v_T$, (iii) $t > t_p$, $v > v_T$; (c) $P=3$, a metastable state.

below which the sliding threshold and multiplicity of solutions disappear,⁹ is immediately seen to be $P_c = 1$.

The threshold force can be determined graphically, using (8), for all P . Further, in the limit $P \rightarrow P_c^+$, the multivalued region in Fig. 1 shrinks towards the origin where (7) gives

$$x - g^3/6 + (P - P_c)g = 0, \quad (9)$$

and (8) gives, with elementary calculus, $f_T = [9/(4\pi)](P - P_c)^{2/3}$ as $P \rightarrow P_c^+$, where $\Psi_T = 2$. For large P one obtains $f_T = P - \pi + O(P^{-1/2})$.

Further, it is immediately clear from Fig. 1(b) that at $f = f_T$ there is only one stationary state,⁴ g_T .

Turning to dc dynamics, $\alpha = v t$ in (6) and g is continuous. As $v \rightarrow 0$, g will approach g_T as $f \rightarrow f_T^+$. It is easy to see from (7) that for x away from the critical value x_T , $g - g_T = 0(v)$. In the vicinity of x_T , putting $x = x_T + y$, $x + g(x) = x_T + g_T(x_T^-) + h(y)$ and considering (7) in the limit of small y and $h(y)$ gives¹⁰ $v dh/dy = y + ah^2$, where $a = -g_T(x_T^-)/2$. Transforming by

$$\frac{dw}{dz} = -\alpha h(\beta z)w(z), \quad (10)$$

where $\alpha = (a^2/v)^{1/3}$ and $\beta = (v^2/a)^{1/3}$ gives $w'' = -zw(z)$, the solutions of which¹¹ are the Airy functions $\text{Ai}(-z)$ and $\text{Bi}(-z)$. The boundary condition that $h(y)$ be finite and negative for $y < 0$ as $v \rightarrow 0$ means, integrating (10), that $w(z) \rightarrow 0$ as $z \rightarrow -\infty$. This eliminates $\text{Bi}(-z)$, which diverges as $z \rightarrow -\infty$. Thus

$$h(y) = \left[\frac{v}{a^2} \right]^{1/3} \frac{\text{Ai}'(-(a/v^2)^{1/3}y)}{\text{Ai}(-(a/v^2)^{1/3}y)},$$

and the limiting value of $y = x - x_T$ for finite h , as $v \rightarrow 0$, is $(v^2/a)^{1/3}z_0$ where z_0 is the first zero of $\text{Ai}(-z)$. This result is seen graphically to give a dominant contribution $\sim v^{2/3}$ to $f - f_T$ in (3). Thus $v = B(f - f_T)^{3/2}$, where $B = [2\pi a^{1/3}/(z_0 \Delta)]^{3/2}$ and $\Delta = g_T(x_T^+) - g_T(x_T^-)$. Further, as $P \rightarrow P_c^+$ using (9) gives

$$B = [2^{1/3}\pi/(3z_0)]^{3/2}(P - P_c)^{-1/2}.$$

Thus the depinning transition, and the $\frac{3}{2}$ threshold exponent with a coefficient which diverges as $P \rightarrow P_c^+$, in agreement with Ref. 4, can be obtained quite straightforwardly for the incommensurate chain. The simplicity of the present calculation is due to the elimination of the center-of-mass coordinate (U) leaving a function of only one variable to be determined in solving incommensurate dc dynamics.

Further, it is possible to determine the energy and stability of each stationary state and thus specify, for $P > P_c$, which is the ground state, which are the metastable states, and which are the unstable states. The energy corresponding to Eq. (1) is

$$H = \sum_j P \cos(H_j + U_j) + (4N)^{-1} \sum_j (U_i - U_j)^2.$$

Using (6) and choosing g to minimize H shows that the ground state has a single discontinuity, which moves from 0 to x_T as f increases from 0 to f_T [Fig. 1(b)].

To distinguish metastable from unstable states the linear stability of stationary solutions $\{U_j\}$ of (1) must be studied. Replacing U_j by $U_j + u_j$ in (1) gives, to $O(u_j)$, \ddot{u}_j

$= (\underline{M}_0 + \underline{M}_1)\ddot{u}_j$, where $M_0^{(j)} = (P \cos(H_j + U_j) - 1)\delta_{jj}$ and $M_1^{(j)} = N^{-1}$. The Green's function $\underline{G}(z) = (z - \underline{M}_0 - \underline{M}_1)^{-1}$ is easily calculable by summing the usual expansion in powers of \underline{M}_1 . With

$$G_0^{(j)}(z) = (z - \lambda_j)^{-1}\delta_{jj}, \quad \lambda_j = P \cos(H_j + U_j) - 1,$$

one obtains $\underline{G} = \underline{G}_0 + \underline{G}_0 \underline{T} \underline{G}_0$, where $T^{(j)} = [N(1 - \mu)]^{-1}$ and $\mu(z) = N^{-1} \sum_j (z - \lambda_j)^{-1}$. Thus the poles of \underline{G} , which are eigenvalues of the stability problem, are the roots of $\mu(z) = 1$. A plot of $\mu(\lambda)$ for real λ then immediately shows¹⁰ that any g which occupies a finite part of the middle branch (dashed line in Fig. 1) will be unstable. Further, as $N \rightarrow \infty$, the largest root of $\mu(z) = 1$ remains an isolated excitation. Transforming sums to integrals, it is straightforward to show that this eigenvalue is negative for any state g which avoids the "unstable" middle branch. Thus any such state which is not the ground state is metastable. An example of a metastable state is shown in Fig. 1(c).

Since the Green's function is known, the exact density of relaxational [(1) is massless] excitations, $\rho(\lambda)$ can be determined in the usual way. For $P < P_c$, transforming sums to integrals, and writing $\bar{\rho}(\lambda) = -\lambda(P^2 - (\lambda + 1)^2)^{-1/2}/\pi$, one obtains for large N

$$\rho(\lambda) = \bar{\rho}(\lambda)\theta(P^2 - (\lambda + 1)^2) + N^{-1}\delta(\lambda),$$

which is shown in Fig. 2(a). The isolated excitation at $\lambda = 0$ is the sliding mode of the unpinned chain.

For $P > P_c$, $f = 0$, the excitation spectrum $\rho(\lambda)$ was determined for the ground state shown as curve (i) in Fig. 1(b). The result for large N is

$$\rho(\lambda) = \bar{\rho}(\lambda)\theta(1 + P + \lambda)\theta(\bar{\lambda}_0 - \lambda) + N^{-1}\delta(\lambda - \bar{\lambda}_p),$$

where $\bar{\lambda}_0 = -1 + P \cos[g(0^+)] < 0$, and $\bar{\lambda}_0 < \bar{\lambda}_p < 0$. This spectrum is shown in Fig. 2(b). As $P \rightarrow P_c^+$, (9) gives $\bar{\lambda}_0 = -2(P - P_c)$. Further, as $P \rightarrow P_c^+$, $\bar{\lambda}_p = -b(P - P_c)$ where b is between 0 and 2 and is the root of

$$\left[\frac{3}{1+b} \right]^{1/2} = \coth \left[\frac{3(1+b)}{b^2} \right]^{1/2}.$$

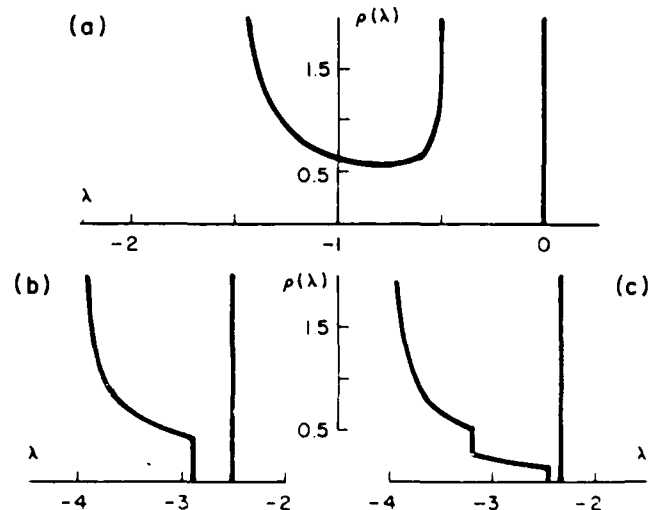


FIG. 2. Excitation spectra $\rho(\lambda)$. (a) $P = 0.5$, $f = 0$; (b) $P = 3$, $f = 0$; (c) $P = 3$, $0 < f < f_T$.

Thus as $P \rightarrow P_c^+$ the gap in the ground-state excitation spectrum closes as $(P - P_c)^{\psi_1}$ where $\psi_1 = 1$.

For $P > P_c$, the excitation spectrum was also determined for $f > 0$. For the ground state shown as curve (ii) in Fig. 1(b), one finds

$$\rho(\lambda) = \begin{cases} \bar{\rho}(\lambda), & -1 - P < \lambda < \bar{\lambda}_+, \\ \bar{\rho}(\lambda)/2, & \bar{\lambda}_+ < \lambda < \bar{\lambda}_-, \\ N^{-1}\delta(\lambda - \bar{\lambda}_f), & \bar{\lambda}_- < \lambda, \end{cases}$$

where $\bar{\lambda}_{\pm} = -1 + P \cos[x_f + g(x_f^{\pm})]$; and $\bar{\lambda}_- < \bar{\lambda}_f < 0$. As $f \rightarrow f_T^-$, $\bar{\lambda}_-(f) = -A(f_T - f)^{1/2}$, where $A(P) \rightarrow (2/3)^{1/2}$ as $P \rightarrow P_c^+$. This spectrum is shown in Fig. 2(c). Further, as

$$f \rightarrow f_T^-, \quad \bar{\lambda}_f = \bar{\lambda}_- + D \exp[-C(f_T - f)^{-1/2}],$$

where $D = 2(P^2 - 1)^{1/2}P$ and $C = [\Delta^2(P^2 - 1)/(4a)]^{1/2}$. That is, as $f \rightarrow f_T^-$, the isolated excitation collapses exponentially rapidly onto the edge of the continuum. Moreover, the gap in the excitation spectrum closes as $(f_T - f)^{\psi_2}$ where $\psi_2 = \frac{1}{2}$.

Finally, knowing the Green's function gives the exact

$$E(z, \lambda) = \frac{2}{[P^2 - (1 - z)^2]^{1/2}} \coth^{-1} \left[\frac{P + 1 - z}{[P^2 - (1 - z)^2]^{1/2}} \frac{P - 1 - \lambda}{[P + 1 + \lambda]^{1/2}} \right].$$

The result (11) may be compared with CDW experiments for both the real and imaginary parts of $\sigma(\omega)$ for all $|f| \leq f_T$ and for all ω . The single-particle model¹² is easily seen to have the property $\lim_{\omega \rightarrow 0} -\text{Im}\sigma/\omega \rightarrow \infty$ as $f \rightarrow f_T$. No such divergence has been observed experimentally.¹³ As $\omega \rightarrow 0$ and $f \rightarrow f_T$, the term in square brackets in (11) becomes

$$\Delta + \frac{i\omega}{(P^2 - 1)^{1/2}} \ln \left(\frac{P(|\bar{\lambda}_-| - i\omega)}{2(P^2 - 1)} \right).$$

While $|\bar{\lambda}_-| \rightarrow 0$ as $f \rightarrow f_T$, the dielectric constant, $\epsilon = i\sigma/\omega$, nevertheless remains finite near f_T even as $\omega \rightarrow 0$. The entire spectral weight of the single-particle model is at one frequency which approaches zero at threshold. The pinned many-body system considered here has a broad spectrum of excitations, only one edge of which approaches zero at threshold. This is the first explicit demonstration that in such a case the singularity in σ is weaker than in the

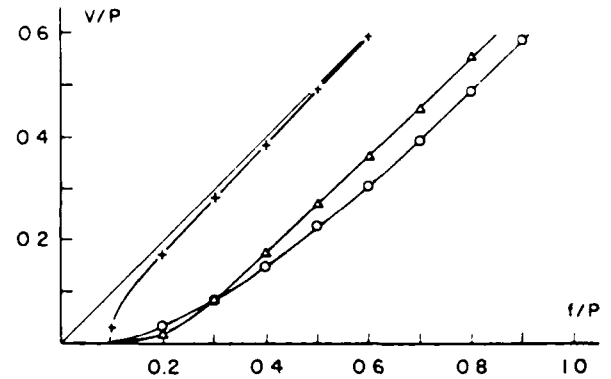


FIG. 3. dc characteristic for $P=1 \times 5$ (O); also (with matched thresholds and large ν slopes) for single-particle model (Ref. 12) (+) and NbSe₃ CDW (Ref. 16) (Δ).

linear ac response of the pinned lattice. For $P > P_c$ the result is

$$\sigma(\omega; f; P) = i\omega [1 - 2\pi \{ \Delta_f - i\omega (E(i\omega, \bar{\lambda}_-) + E(i\omega, \bar{\lambda}_+)) \}^{-1}], \quad (11)$$

where $\Delta_f = g(x_f^+) - g(x_f^-)$ and

single-particle case and ϵ can remain finite, as is observed experimentally.¹³

For nearest-neighbor interactions, the ground state g is more singular and some numerical determinations of depinning exponents for a stationary center of mass have been made.^{9,14} Equation (1) can be considered a mean-field theory for the incommensurate chain with finite-range interactions. The present straightforward solution may be useful in the ultimate analytic solution of sliding threshold dynamics with short-range interactions. For constant $f > f_T$ outside the threshold region, the truncation procedure of Ref. 2 gives an accurate solution of Eq. (1), including the response to small ac perturbations. As seen for example¹⁵ in Fig. 3, this combines with the present results for $f \leq f_T$ to give a complete steady-state solution of this system.

The author thanks E. Gross for stimulating discussions and the Air Force Office of Scientific Research for support under Grant No. 84-0014.

¹P. Bak, Rep. Prog. Phys. **45**, 587 (1982).

²L. Sneddon, Phys. Rev. Lett. **52**, 65 (1984).

³L. Sneddon, Phys. Rev. B **29**, 719 (1984).

⁴D. S. Fisher, Phys. Rev. Lett. **50**, 1486 (1983).

⁵This periodicity can be seen to hold to all orders of perturbation in P .

⁶An alternative elimination of $\langle U \rangle$ was given in Ref. 2.

⁷Such solutions were seen in the truncation procedure of Ref. 2 to be dynamically stable and to match CDW properties in TaS₂.

⁸Equation (6) was obtained by Aubry (see Ref. 9) for static ($\alpha = 0$) solutions of the nearest-neighbor chain, and can be seen here and in Ref. 2 to describe dc dynamics ($\alpha \neq 0$) and arbitrary-range interactions as well. Infinite-range interactions are easier because with finite-range interactions, Eqs. (4) and (7) become differential

difference equations.

⁹M. Peyrard and S. Aubry, J. Phys. C **16**, 1593 (1983), and references therein.

¹⁰ $dq_T/dx \rightarrow \infty$ as $x \rightarrow x_T^-$ so $P \cos[x_T + q_T(x_T^-)] = 1$.

¹¹M. Abramowitz and I. A. Stegun, *Handbook of Mathematical Functions* (U.S. GPO, Washington, D.C. 1964).

¹²G. Grüner, A. Zawadowski, and P. M. Chaikin, Phys. Rev. Lett. **46**, 511 (1981).

¹³A. Zettl and G. Grüner, Phys. Rev. B **29**, 755 (1984).

¹⁴S. J. Shenker and I. P. Kadanoff, J. Stat. Phys. **27**, 631 (1982).

¹⁵The pinning strength was chosen to be the same as in Ref. 2, and not as a best fit in Fig. 3.

¹⁶R. M. Fleming, Phys. Rev. B **22**, 5606 (1980).

PUBLICATION 3.

Electromechanical Properties of Charge-Density-Wave Conductors

Leigh Sneddon

Department of Physics, Brandeis University, Waltham, Massachusetts 02254

(Received 31 October 1985)

A model of two mutually incommensurate, interacting, dynamical, many-body systems is presented and solved. Quasiperiodic forms are shown to describe both the dc properties and the complete set of linear excitations. By use of one system to represent the crystal lattice and the other a charge-density wave (CDW), all the recently discovered, and as yet unexplained, electromechanical properties of CDW conductors are shown to occur in this model. The internal degrees of freedom of the CDW are shown to be of central importance.

PACS numbers: 72.15.Nj, 72.15.Eb, 72.20.Ht

Until recently the widespread interest in charge-density-wave (CDW) conductors has centered on their nonlinear electrical properties.¹ Elegant experiments by Brill and Roark² and by Mozurkewich *et al.*,³ however, have now shown that the motion of a CDW also changes the mechanical properties of the host crystal. Speculation as to the origin of these phenomena has included CDW domain-wall relaxation² and phason-phonon interactions³; and a satisfactory calculation of the current dependence of mechanical properties is still lacking.

This Letter addresses the question of whether single-domain, noncommensurate, classical, many-body models, which have exhibited a variety of non-

linear electrical properties of CDW's⁴⁻⁶ (e.g., dc characteristics, ac response, ac-dc interference, and voltage fluctuations) can also give a satisfactory account of these new electromechanical properties. A model is solved which includes both the host-crystal degrees of freedom and the internal degrees of freedom (IDF's) of the CDW. It consists of two interacting mutually incommensurate chains, one representing the crystal lattice and the other the CDW. Conservative and viscous interactions between the chains are used to represent respectively the pinning force which produces the CDW threshold, and the dissipation which results from CDW motion through the crystal.

Dimensionless classical equations of motion for this model can be written:

$$m\ddot{\Phi}_\alpha + \sum_\beta \Delta_\beta \Phi_{\alpha-\beta} + \mu \sum_j W(X_{\alpha j})(\dot{\Phi}_\alpha - \dot{U}_j) = -\mu \sum_j F(X_{\alpha j}) - E_L, \quad (1)$$

$$\sum_p D_p U_{j-p} + \sum_\alpha W(X_{\alpha j})(\dot{U}_j - \dot{\Phi}_\alpha) = \sum_\alpha F(X_{\alpha j}) + E, \quad (2)$$

where m is the ionic mass, the inertia of the CDW is negligible, Φ_α and U_j are the displacements of particle α in the crystal lattice and particle j in the CDW, respectively, and $2\pi\alpha$ and Hj are their respective undisplaced positions, so that

$$X_{\alpha j} \equiv 2\pi\alpha + \Phi_\alpha - [Hj + U_j] \quad (3)$$

is the distance between them. The coefficients Δ_β and D_p are the spring constants of internal, harmonic restoring forces in the lattice and the CDW, respectively. The function $W(x)$ is a weighting function centered at $x=0$, and represents the spatial range of the dissipative interactions. The force F between particles α and j also depends on their separation $X_{\alpha j}$. E is the electric field acting on the CDW and $-E_L$ is the force which keeps the lattice stationary. The incommensurate limit is approached by a consideration of M particles in the crystal lattice chain, N in the CDW chain, and $M/N = H/2\pi \rightarrow$ a fixed irrational. The parameter μ is a formal expansion parameter ultimately to be set equal to 1. This model thus treats the lattice and the CDW as two separate entities, each distorting the other.⁷ In

the stiff-lattice limit ($\Delta \gg F$), $\Phi_\alpha = \langle \Phi_\alpha \rangle$,⁸ and the crystal lattice simply produces a rigid incommensurate potential through which the CDW moves, exhibiting a variety of experimentally observed nonlinear electrical properties.⁴⁻⁶

The first general result, which can be checked by substitution for any Δ , is that stationary states, and states of dc relative motion of the centers of mass of the two interacting chains, are described by quasiperiodic forms

$$\begin{aligned} \Phi_\alpha(t) &= Q(y), & U_j(t) &= vt + G(x), \\ y &= 2\pi\alpha - vt, & x &= Hj + vt, \\ Q(y+H) &= Q(y), & G(x+2\pi) &= G(x), \end{aligned} \quad (4)$$

where $v = \langle \dot{U}_j \rangle$, the CDW center-of-mass velocity. Thus the quasiperiodic form first shown to describe the *statics* of a single incommensurate chain,⁹ and subsequently shown to describe its dc dynamics as well,⁴ is now seen to describe *both* the statics and dc dynamics of two interacting dynamical systems.

Further, the linear fluctuations of the dual interacting system, both when static and when undergoing dc relative motion, are likewise characterized by quasi-periodic forms. If $\phi_\alpha = \bar{\phi}_\alpha \exp(-i\omega t)$ and $u_j = \bar{u}_j \exp(-i\omega t)$ are fluctuations in the crystal lattice and CDW chains, respectively, a complete set of linear fluctuations is given by

$$\begin{aligned} \bar{\phi}_\alpha(t) &= e^{iq2\pi\alpha} r(y), & \bar{u}_j(t) &= e^{iqx} h(x), \\ r(y+H) &= r(y), & h(x+2\pi) &= h(x), \end{aligned} \quad (5)$$

where x and y are as in (4). The normal modes of the dual interacting system thus resemble Bloch waves.¹⁰ If the two chains do not interact, r and h are constant and the excitations are simple traveling waves. Inter-chain interactions produce a quasiperiodic modulation of each wave. In the special case of the stiff-lattice limit these excitations reduce to those of incommensurate single-chain systems, which have been studied numerically in the static case ($v=0$)⁹. We now see that these excitations are "quasiperiodic Bloch waves." Further, the exponential factors in ϕ_α and u_j are waves with phase velocities, respectively, of ω/q in the crystal lattice and $\omega/q - v$ in the CDW. Since the CDW is traveling at v relative to the crystal, both waves are traveling at the same velocity in the laboratory frame.

To compare the properties of this model with experimental data, a small force $f_\alpha e^{-i\omega t}$ will be considered to act on the crystal, and the resonant frequency, ω_0 , defined as the frequency at which the driving and the displacement are $\pi/2$ out of phase,² will be determined as a function of the voltage across the system. The in-

verse displacement amplitude at resonance is then a measure² of "internal friction," Q^{-1} .

Since the effect of the CDW on the Young's modulus is of the order of a percent,² Eqs. (1) and (2) will be studied as an expansion about the stiff-lattice limit. This is most clearly done by expansion of the solution in powers of the formal parameter μ , which premultiplies the forces distorting the lattice.

The calculation begins by replacement of U_j by $U_j + \bar{u}_j(t)e^{-i\omega t}$, Φ_α by $\Phi_\alpha + \bar{\phi}_\alpha(t)e^{-i\omega t}$, and $-E_L$ by $-E_L + f_\alpha e^{-i\omega t}$ in Eqs. (1) and (2), of which the U_j 's and Φ_α 's form a dc solution; retention of only terms linear in \bar{u} , $\bar{\phi}$, and f ; and consideration of $\bar{\phi}_\alpha$ of the form, to $O(\mu^0)$, of a normal mode, i.e.,

$$\bar{\phi}_\alpha = \exp(iq2\pi\alpha). \quad (6)$$

Multiplied throughout by $\exp(-iq2\pi\alpha)$, and averaged over α , Eq. (1) then gives

$$f + m\omega^2 - \Delta(q) = \mu M^{-1} \sum_{\alpha j} Z_{\alpha j} \equiv \delta f, \quad (7)$$

where¹¹

$$Z_{\alpha j} = [F'(X_{\alpha j}) - i\omega W(X_{\alpha j})](1 - \bar{u}_j e^{-iq2\pi\alpha}). \quad (8)$$

To determine f to $O(\mu)$ in (7) only requires that $Z_{\alpha j}$, and hence U_j , Φ_α , and u_j , be determined to $O(\mu^0)$, i.e., in the rigid-crystal-lattice limit, for which we may put $\Phi_\alpha = \langle \Phi_\alpha \rangle = 0$. To determine U_j and u_j , the case of infinite-range internal CDW interactions⁵ ("mean field theory") will be considered: $\sum_p D_p U_{j-p} = U_j - \langle U \rangle$. Use of Eqs. (3)-(6) and linearizing of (2) then gives (for $q \neq 0$ so that $\langle u_j \rangle = 0$)

$$v \sum_\alpha W(X_\alpha) h'(x) + [1 + \sum_\alpha \{C_\alpha + iqv W(X_\alpha)\}] h(x) = \sum_\alpha C_\alpha \exp[iq(2\pi\alpha - x)], \quad (9)$$

where $X_\alpha = 2\pi\alpha - x - g(x)$, $C_\alpha = F'(X_\alpha) - i\omega \times W(X_\alpha) - v W'(X_\alpha)[1 + g'(x)]$, and $g(x)$ is the solution to

$$g(x) + v \sum_\alpha W(X_\alpha)[1 + g'(x)] = \sum_\alpha F(X_\alpha), \quad (10)$$

subject to $g(x+2\pi) = g(x)$. [The electric field E is given by $-(2\pi)^{-1} \int_{-\pi}^{\pi} dx g(x)$.]

Equations (9) and (10) were solved numerically and the results used with (5), (7), and (8) to determine δf above threshold. Below threshold, Eq. (2) was integrated numerically to a stationary state and then linearized to calculate δf to $O(\mu)$ in (7). Since the relative shift in resonant frequency is small, the real and imaginary parts of δf directly give $\Delta\omega_0^2$ and Q^{-1} , respectively, each to within a multiplicative constant. These quantities are shown in Fig. 1 as a function of voltage, or E . W was chosen to be a Gaussian of height 1 and width 6 and F had a maximum value of 2.2 and resulted from a repulsive Gaussian potential of width 3, with $q = \frac{1}{33}$ and $\omega = 0.12$.

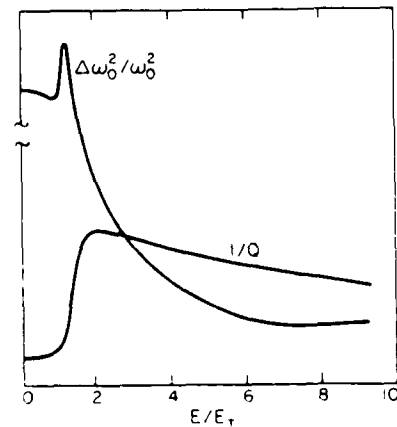


FIG. 1. Electromechanical properties of the incommensurate lattice-CDW model: relative shift in the Young's modulus ($\Delta\omega_0^2/\omega_0^2$) and internal friction (Q^{-1}), both plotted in arbitrary linear units.

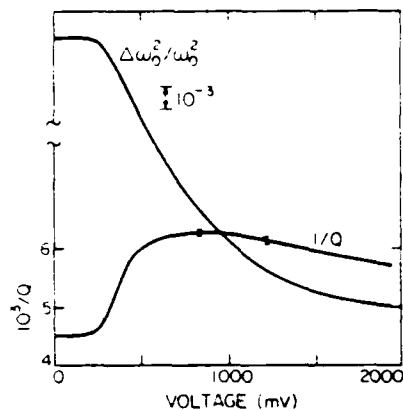


FIG. 2. Electromechanical properties of TaS₃ at 96 K (Ref. 12). The vertical bars indicate the maximum scatter in the data points.

Experimental results¹² are shown in Fig. 2. The calculated $\Delta\omega_0^2$ reproduces the general form of the data. It also contains a peak, however, which is not apparent in these data, although much smaller peaks have now been seen in some samples.^{12,13} This difference between theory and experiment may be due, for example, to the existence of a phason gap in the mean-field theory (see below), to the one-dimensionality of the model, or to inhomogeneities in the crystal.

The rapid rise of Q^{-1} above threshold is clearly seen, with Q^{-1} reaching a maximum well before ω_0^2 has leveled off, a feature emphasized in the original experimental report.² The gradual decline of Q^{-1} at higher voltages was not reported prior to these calculations, and has by now been repeatedly observed.^{12,13}

A qualitative interpretation of the Young's-modulus results is that, for small q , the rigidity of a CDW pinned to a lattice enhances the rigidity of the lattice. For fields larger than threshold, this mechanical coupling of the two systems,^{14,15} and hence the enhancement of the Young's modulus, diminishes.

This decoupling of the sliding CDW from the lattice excitations can be demonstrated particularly dramatically with the choice of infinite-range CDW internal interactions. In this case the CDW's bare excitation (phason) spectrum has a gap: $\omega_{\text{phason}} \neq 0$ as $q \rightarrow 0$. When the CDW is pinned to the lattice this results in a gap in the spectrum of the combined lattice-CDW system. [This was checked numerically by determining that $\delta f(\omega, q \rightarrow 0) \neq 0$ below threshold.] Above threshold, comparison of (9) to the negative of the derivative of (10) with respect to x shows that $h(x) \rightarrow -g'(x)$ as $q, \omega \rightarrow 0$. Use of (4), (5), (7), and (8) then gives

$$\delta f(q, \omega \rightarrow 0) \propto \int_{-\pi}^{\pi} dx \left(\frac{d}{dx} \right) \sum_{\alpha} F(2\pi\alpha - x - g(x)) = 0,$$

since g is periodic and continuous above threshold. Thus the rigidity of the CDW is coupled strongly to the lattice below threshold, in this case producing a gap, but less strongly above threshold, as indicated here by the disappearance of the gap.¹⁶

When we turn to the internal friction, below threshold many IDF's are suppressed by the pinning, while above threshold more can be excited. These dissipate energy and enhance Q^{-1} . As the CDW velocity increases further, however, the coupling between the lattice and the CDW weakens and the excitation of IDF's, and hence Q^{-1} , decreases slowly.

The importance of CDW IDF's can also be demonstrated by our leaving them out, for example, by making the CDW stiffness coefficients D_p in (2) very large, so that $U_j - \langle U \rangle$ and u_j vanish. One then recovers a model similar to that studied¹⁷ to illustrate a symmetry-breaking effect of the CDW current. From (7) and (8), δf in this limit is, to $O(\mu)$, $-i\omega(2\pi)^{-1} \int_{-\pi}^{\pi} dx \sum_{\alpha} W(2\pi\alpha - x)$, a constant. Thus to $O(\mu)$ a rigid CDW produces no voltage dependence in the crystal's mechanical properties; hence, the effects calculated in Ref. 17 were $O(\mu^2)$. The presence of IDF's, however, allows a *first-order* contribution, as shown in Fig. 1. Since the crystal lattice is much stiffer than the CDW, first-order effects are much larger than second-order effects, and IDF's of the CDW thus produce voltage-dependent shifts in mechanical properties of magnitude larger than those predicted with no IDF's.

The dependence of lattice properties on the CDW velocity, v , is also of interest. Without IDF's the sound velocity, s , is found¹⁷ to be an analytic function of v at $v=0$, with an antisymmetric, linear leading term and higher-order corrections that are much smaller if, as is the case in CDW experiments, $v \ll s$. The enhancement of the Young's modulus studied in this Letter, however, will produce a symmetric v -dependent component¹⁸ in $s(v)$, which should therefore deviate from antisymmetry over observable CDW velocity scales much less than s . The inclusion of IDF's also results in the $v \rightarrow 0$ limit being a singular limit, the threshold at which, for example, the electric field is related to v in a nonanalytic fashion,⁵ and the function g becomes singular. It is thus possible that δf in (7), and hence the sound velocity, will also be non-analytic functions of v . Thus, in addition to strongly enhancing the current-induced shifts in lattice properties, the CDW IDF's will contribute a significant symmetric component to, and possibly also change the analyticity of, the sound velocity as a function of CDW current.

A single-domain, incommensurate, classical, many-body model of the type that has exhibited a variety of electrical properties of CDW conductors^{4,6} has been solved and seen to account for electromechanical prop-

erties as well. As is the case for the electrical properties, the internal degrees of freedom^{14,15} of the CDW were seen to play an essential role.

I wish to thank J. W. Brill, K. A. Cox, M. C. Cross, E. P. Gross, and A. C. Lilly for stimulating conversations, and R. J. Maher and A. D. Zima for assistance with a Gould computer. I am grateful for the hospitality of the Philip Morris Visiting Scientist Program, during which this work was completed, and to the U.S. Air Force Office of Scientific Research for support under Grant No. NP-84-0014.

¹See *Charge Density Waves in Solids*, edited by G. Hutiray and J. Solyom, Lecture Notes in Physics Vol. 217 (Springer-Verlag, New York, 1985).

²J. W. Brill and W. Roark, *Phys. Rev. Lett.* **53**, 846 (1984).

³G. Mozurkewich, P. M. Chaikin, W. G. Clark, and G. Grüner, in Ref. 1, p. 353.

⁴L. Sneddon, *Phys. Rev. Lett.* **52**, 65 (1984).

⁵L. Sneddon, *Phys. Rev. B* **30**, 2974 (1984).

⁶L. Sneddon and K. Cox, to be published.

⁷Related models have been studied in zero-current states by use of continuum approximations and/or a rigid-lattice limit: See, e.g., G. Theodorou and T. M. Rice, *Phys. Rev. B* **18**, 2840 (1978); T. Ishii, *J. Phys. Soc. Jpn.* **52**, 168 (1983); T. Munakata, *J. Phys. Soc. Jpn.* **52**, 1653 (1983).

⁸Angular brackets denote an instantaneous average over the appropriate chain.

⁹M. Peyrard and S. Aubry, *J. Phys. C* **16**, 1593 (1983), and references therein.

¹⁰Similar forms describe electrons in a quasiperiodic potential [S. Ostlund, R. Pandit, D. Rand, H. Schellnhuber, and E. Siggia, *Phys. Rev. Lett.* **50**, 1873 (1983), and references

therein]. This problem is related to the linear excitations of a static single incommensurate chain. A similar form was also found by Ishii (Ref. 7).

¹¹In arriving at Eq. (8), we have eliminated a term

$$(\partial/\partial t)\{W(X_{n_j})[1 - \bar{u}_j \exp(-iq2\pi\alpha)]\}.$$

When $v=0$ it vanishes. When $v \neq 0$, its contribution to the sum in (7) can be seen still to vanish as follows: Using (3), (4), and (5), and writing $x_j = Ht - vt$, we can write this contribution in the form

$$\begin{aligned} & \mu M^{-1}(\partial/\partial t) \sum_j Y(x_j) \\ & = \mu N(2\pi M)^{-1}(\partial/\partial t) \int_{-\infty}^{\infty} Y(x) dx = 0, \end{aligned}$$

where $Y(x+2\pi) = Y(x)$. Such a sum can be replaced by the integral, here and subsequently, because $H/2\pi \rightarrow$ an irrational.

¹²J. W. Brill, W. Roark, and G. Minton, to be published.

¹³A. Zettl, private communication.

¹⁴L. Sneddon, M. C. Cross, and D. S. Fisher, *Phys. Rev. Lett.* **49**, 292 (1982).

¹⁵L. Sneddon, *Phys. Rev. B* **29**, 719 (1984). The flow of normal current to screen charge fluctuations due to IDF's was considered here and shown to produce an enhancement of CDW damping with decreasing temperature in semiconductors. This prediction was recently confirmed experimentally by R. M. Fleming, R. J. Cava, L. F. Schneemeyer, E. A. Reitman, and R. G. Dunn (to be published).

¹⁶This demonstration is to $O(\mu)$, it can be shown to all orders that the gap vanishes for $v \neq 0$.

¹⁷S. N. Coppersmith and C. M. Varma, *Phys. Rev. B* **30**, 3566 (1984).

¹⁸The relative size of the symmetric and antisymmetric parts of $s(v)$ must await a solution with finite-range CDW restoring forces, and hence no $v=0$ gap. The author is grateful to S. N. Coppersmith and C. M. Varma for a discussion of these issues.

PUBLICATION 4.

Oscillatory Instability in the Dynamics of Incommensurate Structures

Leigh Sneddon

Martin Fisher School of Physics, Brandeis University, Waltham, Massachusetts 02254

and

Kenneth A. Cox

Philip Morris Research Center, Richmond, Virginia 23261

(Received 27 March 1985)

We report the discovery of an oscillatory instability in the dynamics of incommensurate structures. The oscillations survive the thermodynamic limit. The instability occurs for both long- and short-range interactions. The frequency and stability of the oscillations are studied.

PACS numbers: 72.70.+m, 72.15.Eb, 72.15.Nj, 72.20.Ht

Quasiperiodic or incommensurate systems have attracted considerable interest in a wide variety of contexts, including adsorbed layers, structures of solids, the onset of chaos, and localization (see, for example, Refs. 1-3). They also exhibit⁴ a variety of the nonlinear properties of sliding charge-density waves (CDW's), including dc characteristics, ac response, ac-dc interference, and electromechanical properties.

We report the discovery of a new phenomenon, a bulk oscillatory instability, in the dynamics of sliding incommensurate structures; and we study some of its properties. The existence of bulk oscillations is surprising since the general belief has been that the phase of any oscillations in a sliding noncommensurate system would vary through the sample, thus cancelling the oscillations in the thermodynamic limit, as indeed occurs in perturbation theory.^{5,6} The instability is therefore breaking the translational symmetry of the bulk noncommensurate system. Finally, in the light of this new result, we discuss the long-standing problem of oscillatory voltage fluctuations in CDW conductors.⁷⁻¹¹

The first model we consider is one for whose dc properties an exact solution is available,⁴ namely, a set of N particles, all interacting equally with each other, subject to a pinning force $P(x)$ and a uniform force F :

$$\dot{U}_j = P(Hj + U_j) + vU_j - U_j + F. \quad (1)$$

Here H is the lattice spacing; U_j is the displacement of the j th particle (so that $Hj + U_j$ is its position); $v = N^{-1} \sum_{j=1}^N \dot{U}_j$; $P(x + 2\pi) = P(x)$; and we study the limit $N \rightarrow \infty$ and $H/2\pi = \text{an irrational}$. Because CDW's are overdamped,^{5,12} purely relaxational dynamics is used. This model can be thought of as a mean-field theory for the incommensurate chain. Following a simple construction¹³ it can be shown, however, that it can also be considered a mean-field theory of a CDW subject to a spatially *random* distribution of identical pinning centers. (With infinite-range interactions, the distinction between the quasiperiodic phase variable Hj and a com-

pletely random phase variable β_j is irrelevant.) It has also provided⁴ accounts of ac-dc interference experiments in the CDW compound TaS_3 , and the scaling of field- and frequency-dependent conductivities.

The exact dc solution of this model is⁴ $U_j(t) = vt + g(Hj + vt)$ where $g(x)$ is the solution of the boundary-value problem

$$v(1 + g') = P(x + g) - g, \quad g(x + 2\pi) = g(x).$$

This solution was used here as the initial configuration for a numerical integration of (1), with N particles, and it was checked that the numerical procedure was stable. By addition of any small perturbation the dynamic stability of this solution can be studied. The voltage (F) versus time plot in Fig. 1 shows the result of such a study. The results presented in Figs. 1 and 2 are¹⁴ for $P(x) = 8\sin x + 12\sin 4x$.

It is immediately apparent that the dc solution is dynamically *unstable*, with oscillatory fluctuations growing exponentially at first and then saturating. The ap-

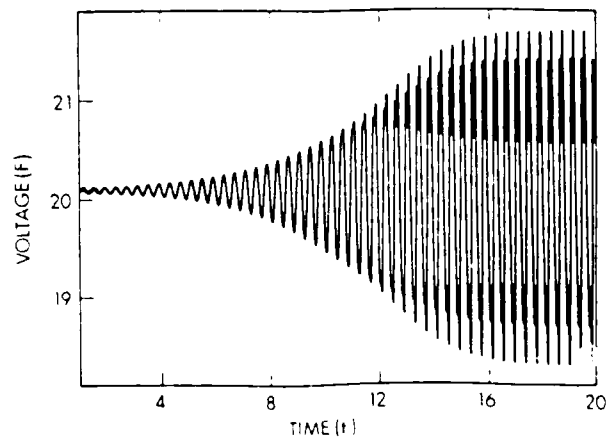


FIG. 1. Voltage vs time for mean-field theory, with $v = 10$. Note the exponential divergence followed by saturation, characteristic of an instability in a nonlinear system.

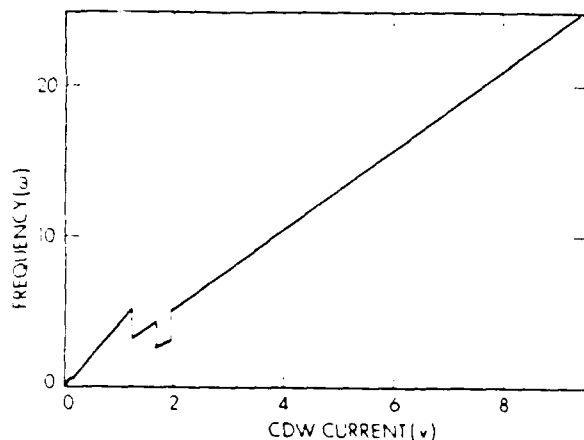


FIG. 2. Frequency vs velocity for the Frenkel-Kontorova model. The segments satisfy $v/\omega = (H/2\pi)^n$ where $n=2$ for the largest segment and cascades through $n=1,2,3,4$ as the velocity is decreased further.

pearance of harmonic content in $F(t)$, as well as saturation, are both due to nonlinearity and they are seen to occur at the same time, as expected. Time series obtained with $N=144, 233$, and 377 are essentially indistinguishable. Thus the results shown in Fig. 1 describe the thermodynamic limit and are not a finite-size effect. Moreover, a finite-size effect would not be expected to show the exponential divergence seen in Fig. 1, which is instead the signature of a dynamic instability.

In addition, we performed a stability analysis of the dc solution to (1) in the limit $N \rightarrow \infty$. CDW experiments are often current driven, and so we considered (1) in the presence of "normal electrons" by keeping fixed a total current, $v + \sigma_n F$, where σ_n is the conductivity of the linear, normal channel. It can be shown that, for any pinning potential, oscillations at (complex) frequency ω will occur under conditions of fixed total current $v + \sigma_n F$ only if ω is a root of $\sigma(\omega) = -\sigma_n$ where $\sigma(\omega)$ is the linear response function of the sliding structure. Thus, while an instability under conditions of fixed voltage F would correspond to a pole of σ crossing into the upper-half complex ω plane, the instability shown in Fig. 1, at fixed current v , corresponds to a zero of σ crossing into the upper-half plane. We solved the linear-response equation and obtained the zeros of σ for different velocities. At $v=10$ the result was a normal-mode frequency whose real and imaginary parts both agreed precisely with the diverging oscillation seen in Fig. 1, confirming that it shows an oscillatory dynamic instability inherent in the mean-field theory of the dynamics of incommensurate structures.

We calculated the complex normal-mode frequency at different velocities. As the velocity decreases below 11, the zero moves into the upper-half complex plane, signaling an instability of bifurcation. There is thus a critical velocity v_c above which the dc solution is stable (oscillations decay) and below which the oscillations persist.

The instability was observed for a wide range of σ_n , with v_c decreasing as σ_n increases.¹⁵

The solution of the linear fluctuation equation at v_c , $\delta U_j t = \eta(Hj + vt)e^{-i\omega t}$, provides some rudimentary insight into the origin of the instability. The exact solution of the dc motion⁴ showed that there are values of the pinning potential (essentially the peak values) which a locally stable static solution avoids by having discontinuities in the function $g(x)$ defined above. Static solutions do exist with particles in these regions, but such solutions are unstable.⁴ A sliding system, however, must have particles in these regions and a continuous $g(x)$, with dg/dx sharply peaked in these regions for small v . We find that the unstable fluctuation $\eta(x)$ has $|\eta|$ largest just where dg/dx is peaked. Thus the oscillatory instability of the dc solution may be in some measure a dynamic consequence of the existence of unstable static states.

To see whether the oscillatory instability exists in finitely coordinated systems we studied a minimally coordinated system: an incommensurate chain with only nearest-neighbor interactions.¹

$$\dot{U}_j = P(H_j + U_j) + U_{j-1} - 2U_j + U_{j+1} + F. \quad (2)$$

The incommensurate chain has been shown⁴ to give an account of the difference between the ac and dc interference properties of NbSe₃ and TaS₃. A previously obtained⁴ dc solution to (2) was used as an initial configuration in a numerical integration with N particles. Increasing N sufficiently produced identical plots, ensuring that the results represented the thermodynamic limit. Different pinning potentials were studied. So long as $P(x)$ produced a threshold, whether or not $P(x)$ contained harmonics, resulting voltage-time plots showed precisely the exponential instability, followed by saturation, that was seen in Fig. 1 for the mean-field case.

Thus the instability occurs at coordination number infinity and two. It is therefore expected to occur in incommensurately pinned systems at all intermediate coordinations in one, two, and three dimensions.

The oscillation frequency as a function of v , for nearest-neighbor interactions and the same $P(x)$ as in Fig. 1, is shown in Fig. 2 and has some interesting features. It is predominantly linear. Further, although the large- v limit has transients with the trivial frequency $\omega = v$ which would be exhibited by a single particle in $P(x)$, once the instability takes over ($v \leq 9$) a new characteristic frequency and length appear which are determined not only by $P(x)$, but also by the sliding structure itself. In the large linear region in Fig. 2, $v/\omega = (H/2\pi)^2$. That is, the oscillatory instability reveals the length scale H provided by the lattice spacing, which is the length scale corresponding to the wavelength of a CDW.

Further, as v is decreased, there are a number of first-order transitions, where v/ω changes abruptly, being

given by $(H/2\pi)^n$, $n=2,1,2,3,\dots$ as the velocity is decreased.

The properties of the Frenkel-Kontorova model [Eq. (2)] have attracted a great deal of attention (see, e.g., Ref. 2). It is now clear that its dynamic properties are considerably richer than previously realized.

Turning to CDW conductors, the dominant source of pinning is believed to be a random potential due to lattice defects. While Eq. (1) is also a mean-field theory of random pinning, we do not yet know whether a bulk oscillatory instability also occurs in systems with random pinning and short-range interactions.

No critical velocity, v_c , has been reported in the experimental literature. Some experiments in the time domain have, however, revealed transient oscillations.¹⁶ While the existence of transients has no clear explanation within the finite-size^{13,17} or contact¹⁸ theories, a natural interpretation in the present context is that in these experiments $v > v_c$ so that fluctuations oscillate but decay.

The origin of CDW voltage oscillations remains an open question. The unexpected observation of bulk oscillations in models which have exhibited a wide variety of other properties of sliding CDW's may be the basis for the answer, or merely a tantalizing coincidence.

In conclusion, we have reported the discovery of new phenomenon—an oscillatory instability—in the dynamics of incommensurate structures.

We wish to thank P. W. Anderson, E. P. Gross, A. J. Kassman, A. C. Lilly, R. J. Maher, P. Monceau, and A. D. Zima for stimulating discussions. One of us (L.S.) is grateful to Philip Morris, Inc., for the hospitality of the Philip Morris Visiting Scientist Program, and to the Air Force Office of Scientific Research for support under Grant No. 84-0014.

¹Y. I. Frenkel and T. Kontorova, *Zh. Eksp. Teor. Fiz.* **18**, 1340 (1938); F. C. Franck and J. H. van der Merwe, *Proc. Roy. Soc. London, Ser. A* **198**, 205 (1949).

²P. Bak, *Rep. Prog. Phys.* **45**, 587 (1982), and references therein, and *Phys. Rev. B* **32**, 5764 (1985); S. J. Shenker and L. P. Kadanoff, *J. Stat. Phys.* **27**, 631 (1982); M. Peyrard and S. Aubry, *J. Phys. C* **16**, 1593 (1983).

³J. M. Greene, *J. Math. Phys.* **20**, 1183 (1979); L. P. Kadanoff, *Phys. Rev. Lett.* **47**, 1641 (1981); M. J. Feigenbaum, L. P. Kadanoff, and S. J. Shenker, *Physica (Amsterdam)* **5D**,

370 (1982); S. J. Shenker, *Physica (Amsterdam)* **5D**, 405 (1982); T. Ishi, *J. Phys. Soc. Jpn.* **52**, 168 (1983); M. Kohmoto, L. P. Kadanoff, and Chao Tang, *Phys. Rev. Lett.* **50**, 870 (1983); S. Ostlund, R. Pandit, D. Rand, H. Schellnhuber, and E. Siggia, *Phys. Rev. Lett.* **50**, 1873 (1983); R. MacKay, Ph.D. thesis, Princeton University, 1982 (unpublished); T. Janssen, in *Incommensurate Phases in Dielectrics*, edited by R. Blinc and A. Levanyuk (North-Holland, Amsterdam, 1986).

⁴L. Sneddon, *Phys. Rev. Lett.* **52**, 65 (1984), and *Phys. Rev. B* **30**, 2974 (1984), and *Phys. Rev. Lett.* **56**, 1194 (1986).

⁵L. Sneddon, M. Cross, and D. S. Fisher, *Phys. Rev. Lett.* **49**, 292 (1982).

⁶The leading order result of Ref. 5 holds to all orders: see L. Sneddon, *Phys. Rev. B* **29**, 725 (1984).

⁷R. M. Fleming and C. C. Grimes, *Phys. Rev. Lett.* **42**, 1423 (1979).

⁸P. Monceau, J. Richard, and M. Renard, *Phys. Rev. Lett.* **45**, 43 (1980), and *Phys. Rev. B* **25**, 948 (1982).

⁹G. Grüner *et al.*, *Phys. Rev. B* **23**, 6813 (1981).

¹⁰P. Monceau *et al.*, *Phys. Rev. B* **28**, 1646 (1983), and references therein.

¹¹See Proceedings of International Symposium on Nonlinear Transport and Related Phenomena in Inorganic and Quasi One-Dimensional Conductors, Hokkaido University, Sapporo, Japan, 1983, edited by Y. Abe *et al.* (to be published), and *Proceedings of the International Conference on Charge Density Waves in Solids, Budapest, 1984*, edited by Gy. Hutiray and J. Sólyom, Lecture Notes in Physics Vol. 217 (Springer-Verlag, New York, 1985).

¹²G. Grüner, L. C. Tippie, J. Sanny, W. G. Clarke, and N. P. Ong, *Phys. Rev. Lett.* **45**, 935 (1980).

¹³D. S. Fisher, *Phys. Rev. Lett.* **50**, 1486 (1983), and *Phys. Rev. B* **31**, 1396 (1985).

¹⁴Harmonic content in $P(x)$ was necessary for the instability to occur with infinite-range interactions but not with finite-range interactions. In all cases we used periodic boundary conditions with $N=N_i$, $H/2\pi=N_{i-1}/N_i-(\sqrt{5}-1)/2$ as $i \rightarrow \infty$.

¹⁵A v_c which vanishes in the fixed-force limit ($\sigma_n \rightarrow \infty$) would explain why studies which were done in this limit did not detect the instability [Ref. 13 and S. N. Coppersmith, *Phys. Rev. B* **30**, 410 (1984)]. In a fixed-voltage or fixed-current experiment the local electric field fluctuates. Whenever, by choosing a_n finite, we allowed f to fluctuate, the dc solution near threshold was unstable and oscillations persisted.

¹⁶M. Oda and M. Ido, *Solid State Commun.* **50**, 879 (1984); R. M. Fleming, L. F. Schneemeyer, and R. J. Cava, *Phys. Rev. B* **31**, 1181 (1985).

¹⁷R. A. Klemm and J. R. Schrieffer, *Phys. Rev. Lett.* **51**, 47 (1983).

¹⁸N. P. Ong, G. Verma, and K. Maki, *Phys. Rev. Lett.* **52**, 663 (1984).

PUBLICATION 5.

Mixing in charge-density-wave conductors

Sen Liu and Leigh Sneadon

The Martin Fisher School of Physics, Brandeis University, Waltham, Massachusetts 02254

(Received 13 November 1986)

Harmonic and direct ac mixing properties of the Fukuyama-Lee-Rice model and the incommensurate chain are determined and compared with experimental data. Field and frequency dependences of both the amplitudes and phases of both of these responses are examined. Agreement with experiment is generally good. For example, classical models can yield low harmonic-mixing quadrature components simultaneously with substantial frequency dependence in both components of the linear response.

An interesting series of experiments, involving the non-linear mixing of ac signals in charge-density-wave (CDW) conductors, was initiated by Seeger, Mayer, and Philipp¹ and thoroughly extended by Miller and co-workers.²⁻⁵ These experiments merit theoretical study in their own right as probes of the unique properties of CDW conductors.

Further, the suggestion has been made that the results "may prove difficult to reconcile with *any* classical theory."⁴ It is thus important to determine the ac mixing properties of classical models of sliding CDW's to see whether there is indeed a failure of the classical picture of bulk CDW motion, and whether these experiments give us evidence for Bardeen's fascinating proposal⁶ that CDW conductors are exhibiting macroscopic quantum tunneling.

The principal experiments²⁻⁵ are direct mixing (or rectification) and harmonic mixing. The sample is driven by a voltage of the form

$$E(t) = E_0 + E_1 \cos(\omega_1 t + \phi) + E_2 \cos(\omega_2 t), \quad (1)$$

where E_1 and E_2 are generally small compared to the threshold voltage E_T . The two measurements consist of detecting the component of the current with frequency ω_0 , where $\omega_0 = \omega_1 - \omega_2$ for direct mixing, and $\omega_0 = 2\omega_1 - \omega_2$ for harmonic mixing. The frequencies are chosen so that ω_0 is much smaller than ω_1 and ω_2 .

The properties of two different models are reported here: the Fukuyama-Lee-Rice (FLR) model⁷ of random pinning and the incommensurate chain.⁸ Perturbation⁹ theory was used to obtain analytic information for the FLR model at large bias fields E_0 . The incommensurate chain was simulated numerically to obtain solutions in the strong-coupling region closer to the sliding threshold field E_T . The equation of motion for the incommensurate chain with infinite-range interactions^{10,11} is

$$\frac{du_j}{dt} = u_j - u_j + P \sin(Hj + u_j) + E(t), \quad (2)$$

where u_j is the displacement of the j th particle, u_c is the center-of-mass displacement, P is the pinning strength, and $H/(2\pi)$ is chosen to be $(\sqrt{5} - 1)/2$.

By simulating Eq. (2) in systems up to 377 particles in size we were able to restrict finite-size effects to the region very close to threshold and ensure that the results obtained at all other fields reliably reflected the thermo-

dynamic limit. The applied frequencies were chosen to have a rational ratio so that the response (in the thermodynamic limit) is periodic. Transients were allowed to decay for a time $t_0 = T$ sufficiently long that $t_0 = T$ and $t_0 = 2T$ give results that are indistinguishable within numerical error. The sampling rate of the time series was chosen high enough that increasing it further produced no noticeable changes.

We now compare the theoretical results with those of experiments, examining each feature of the data in turn.

I. HARMONIC-MIXING PHASE SHIFT

The experimental result which has been most emphasized^{2,4,5} is the failure of some experiments to observe an "internal" phase shift in the small difference-frequency harmonic-mixing response. Classical models were conjectured² to yield nonzero phase shifts at high applied frequencies ω_1 . Wonneberger¹² then showed that the classical single-particle model exhibits a zero phase shift for all ω_1 at large dc bias fields. He proved this result to leading order in perturbation theory and argued in an appendix that the result is valid everywhere above threshold. Nonetheless, it was claimed that the nonobservation of a phase shift above threshold, where *in addition* both components of the *linear* ac response have substantial frequency dependence, may be difficult to reconcile with any classical theory.⁴ It was further claimed that this experimental observation provided particularly significant evidence for CDW tunneling.⁷

We determined the harmonic-mixing properties of the FLR model using perturbation theory at large dc bias fields. The principal result is¹³ that the response component at frequency ω_0 is proportional to $\cos(\omega_0 t + 2\phi)$ in the limit of small ω_0 for large dc bias fields E_0 and all ω_1 . The sine component vanishes linearly with ω_0 . Thus the classical FLR model also exhibits a zero internal phase shift at large bias fields.

In that region, however, the linear ac response has no strong frequency dependence. It is therefore necessary to probe the region of lower dc bias closer to threshold. For this purpose, we turn to the results for the incommensurate chain.

Figure 1 shows some typical field and ω_0 dependences of both components of the harmonic-mixing signal. It is seen that the out-of-phase component is considerably

for the incommensurate chain. Figure 2(b) shows the experimental data,^{2,4} and Fig. 2(c) shows the results^{2,4} which have been presented based on quantum tunneling arguments.

(a) *The peaks.* In Fig. 2(a), the positions (fields) and the heights of the peaks change in the same sense with frequency as seen experimentally. The present results for the incommensurate chain change somewhat more rapidly with frequency than do the experimental data.

(b) *The threshold.* The incommensurate chain is seen in Figs. 2(a) and 2(b) to give the experimentally observed qualitative forms in the vicinity of threshold. The threshold-lowering effect of an applied ac field is also apparent in the incommensurate chain results, the effect increasing as the ac frequency decreases, as observed experimentally.¹⁹

A comparison with Fig. 2(c) then shows that these threshold features reveal substantial differences between the properties of the classical chain and the results of the quantum tunneling analysis.

(c) *The negative dips.* The experimental data [see Fig. 2(b)] show that for lower frequencies ω_1 the harmonic-mixing response goes negative above a (frequency-dependent) field (the phase switches rapidly from a value at or near zero to one at or near 180°). Thereafter the response approaches zero from below. Above a certain frequency, however, this no longer happens and the harmonic-mixing response is always positive.

This points up another qualitative difference between the two sets of theoretical results: While the incommensurate chain, like the experimental results, shows an ω_1 above which the response no longer changes sign, the quantum tunneling analysis appears to show a sign change for all ω_1 .

(d) *Below threshold.* The calculated amplitude of the harmonic-mixing signal is about two or three orders of magnitude less than the peak above threshold, which is consistent with the experimental data [see Fig. 2(b)].

III. DIRECT-MIXING PHASE

Experimentally,^{2,4} the response at $\omega_0 = \omega_1 - \omega_2$ to the cosine input signal of Eq. (1) is found to be proportional to $\cos(\omega_0 t + \phi)$ for small ω_0 . A leading-order perturbative solution of the F1R model¹³ showed this same feature. This conclusion can be seen to be true to all orders as follows. Consider the case $\phi = 0$. Equation (1) is then symmetric with respect to interchanging ω_1 and ω_2 . The total response current at frequency plus or minus ω_0 , J_{DM} , then also has this symmetry. Writing $j_{DM} = I_c \sin(\omega_0 t) + I_c \cos(\omega_0 t)$ then requires $I_c(\omega_1, \omega_2) = -I_c(\omega_2, \omega_1)$, so that $I_c \rightarrow 0$ as $\omega_1 \rightarrow \omega_2$. Even if the input fields are changed to sines by shifting the origin of time, the low-frequency direct-mixing response is still cosine.

IV. DIRECT-MIXING MAGNITUDE

Figure 3(a) shows field and frequency dependence of the magnitude of the direct-mixing response for the incommensurate chain. Figure 3(b) shows the corresponding experimental data. The principal features of the ex-

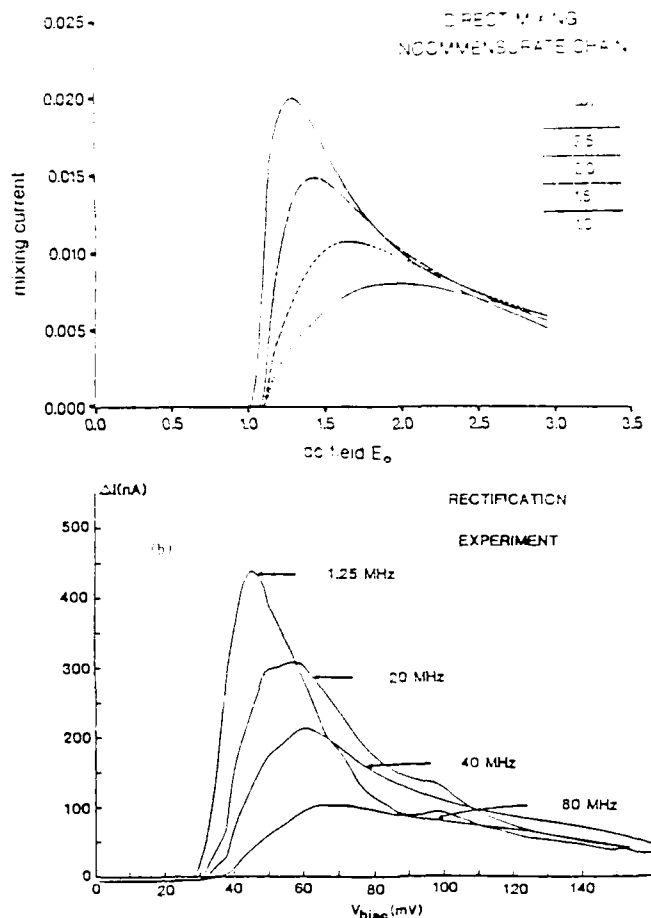


FIG. 3. dc field (E_0) and frequency (ω_1) dependencies of the direct-mixing current ($N^{-1} \sum_j du_j/dt$) magnitude: (a) the incommensurate chain, $N=233$, $P=3.0$, and $E_1=E_2=0.30$; (b) experiment (Ref. 2).

perimental data are seen to be reasonably well reproduced by the incommensurate chain.

V. CONCLUSION

The classical incommensurate chain has been seen to provide a fairly complete account of the field and frequency dependencies of both amplitude and phase components of the direct and harmonic-mixing responses of sliding CDW's.

For example, the challenge to classical theories posed² by some nonobservations of the harmonic-mixing phase shift has been resolved by the observations that (a) phase shifts have been seen experimentally, and (b) classical theories can account for phase shifts as small as the experimental uncertainties. It may be interesting now to have both experimental and theoretical phase shifts determined more precisely to provide more telling comparisons of theories and experiment.

The pinning of CDW's is believed to be due to random impurities,⁷ and not to a periodic incommensurate potential. To end on a question, then, we note that the issue of why incommensurate systems reproduce such a variety of observed CDW properties is still not properly understood.

ACKNOWLEDGMENTS

We are grateful for support from the Air Force Office of Scientific Research, Grant No. 84-0014. This research was supported in part by the National Science Foundation under Grant No. PHY82-17853, supplemented by funds from the National Aeronautics and Space Administration.

-
- ¹K. Seeger, W. Mayer, and A. Philipp, *Solid State Commun.* **43**, 113 (1982).
²J. H. Miller, Jr., J. Richard, J. R. Tucker, and John Bardeen, *Phys. Rev. Lett.* **51**, 1592 (1983).
³J. H. Miller, Jr., J. Richard, R. E. Thorne, W. G. Lyons, J. R. Tucker, and John Bardeen, *Phys. Rev. B* **29**, 2328 (1984).
⁴J. H. Miller, Jr., R. E. Thorne, W. G. Lyons, J. R. Tucker, and J. Bardeen, *Phys. Rev. B* **31**, 5229 (1985).
⁵R. E. Thorne, J. H. Miller, Jr., W. G. Lyons, J. W. Lyding, and J. R. Tucker, *Phys. Rev. Lett.* **55**, 1006 (1985).
⁶See, for example, J. Bardeen, *Phys. Rev. Lett.* **55**, 1010 (1985).
⁷H. Fukuyama and P. A. Lee, *Phys. Rev. B* **17**, 535 (1978); P. A. Lee and T. M. Rice, *ibid.* **19**, 3970 (1979).
⁸Y. I. Frenkel and T. Kontorova, *Zh. Eksp. Teor. Fiz.* **8**, 1340 (1938); F. C. Frank and J. H. van der Merme, *Proc. R. Soc. London, Ser. A* **198**, 205 (1949).
⁹A. Schmid and W. Hauger, *J. Low Temp. Phys.* **11**, 667 (1973); L. Sneddon, M. C. Cross, and D. Fisher, *Phys. Rev. Lett.* **49**, 292 (1982); L. Sneddon, *Phys. Rev. B* **29**, 719 (1984); **29**, 725 (1984).
¹⁰Leigh Sneddon, *Phys. Rev. B* **30**, 2974 (1984). The effects of finite-range interactions will be discussed in Ref. 13.
¹¹L. Sneddon, *Phys. Rev. Lett.* **52**, 65 (1984).
¹²W. Wonneberger, *Z. Phys. B* **53**, 167 (1983).
¹³For details, see S. Liu and L. Sneddon (unpublished).
¹⁴Given Wonneberger's results and conjecture in Ref. 12, the classical single-particle model may also exhibit these properties. We have performed numerical calculations on this model. The results suggest a phase shift which decays linearly with ω_0 , and are thus consistent with Wonneberger's conjecture.
¹⁵J. Richard, R. E. Thorne, W. G. Lyons, J. H. Miller, Jr., and J. R. Tucker, *Solid State Commun.* **52**, 183 (1984).
¹⁶G. Grüner, W. G. Clark, and A. M. Portis, *Phys. Rev. B* **24**, 3641 (1981).
¹⁷This means that the "phase shift" depends on the choice of input signal.
¹⁸N. P. Ong, J. W. Brill, J. C. Ecket, J. W. Savage, S. K. Khanna, and R. B. Somoano, *Phys. Rev. Lett.* **42**, 811 (1979).

smaller than the in-phase component, but appears to be approaching a nonzero limit as ω_0 approaches zero. As ω_0 decreases through 0.05, 0.025, and 0.0125 the out-of-phase component shows practically no change on the scale of the plot.

This limit is generally small. For the data shown in Fig. 1, ω_0/ω_1 is about 0.01, it corresponds to a phase shift of about 10° , which is the reported resolution of the experiments.^{4,5} Experimentally ω_0/ω_1 was chosen to be about 0.001. We found that this phase shift decreases as E_1 and E_2 are increased with the other parameter fixed. The value of ω_1 in Fig. 1 was chosen approximately to maximize the phase shift.

Earlier work¹¹ has established substantial frequency dependence in both components of the linear ac response in this region. One may thus conclude that classical theories can indeed account for the absence of strong quadrature in the harmonic mixing and simultaneous presence of strong frequency dependence in the linear response.¹⁴

The above classical results do appear to show a nonzero quadrature, however, and if a classical picture were appropriate, one would expect to see a phase shift under some experimental conditions. A harmonic-mixing phase shift has, in fact, been reported.¹⁵ The ratios E_1/E_T and E_2/E_T were smaller than in the experiments^{2,3} that saw no phase shift. This is consistent with our observation above that the phase shift decreases as E_1 and E_2 increase.

Turning to the region below threshold, the calculated out-of-phase component is found to be much larger than the in-phase one for small ω_0 . This is consistent with experimental reports⁴ of an internal phase shift of about $\pi/2$.

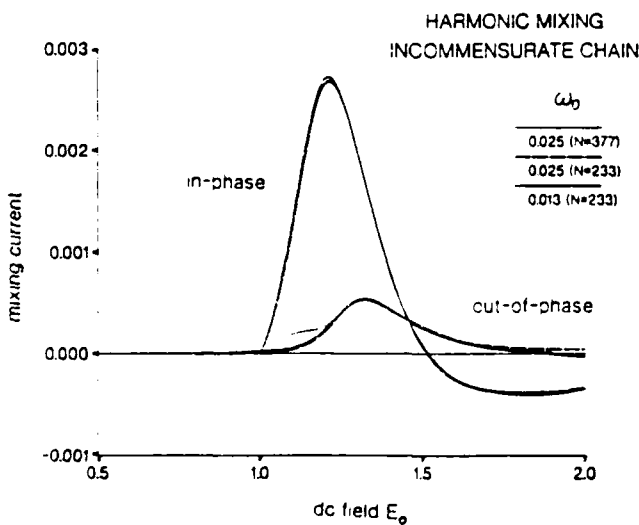


FIG. 1. dc field (E_0) and difference-frequency (ω_0) dependencies of both components of the harmonic-mixing response current ($N^{-1} \sum_j d_i u_j dt$) of the incommensurate chain ($\omega_1 = 1.0$, $P = 3.0$, and $E_1 = E_2 = 0.2$). All quantities are dimensionless [see Eq. (2)]. The curves for $N = 377$ indicate the size of truncation error. Both components have finite $\omega_0 \rightarrow 0$ limits, with the out-phase response considerably smaller than the in-phase response.

II. HARMONIC-MIXING MAGNITUDE

Since the harmonic-mixing phase shift is generally small, we focus now on the magnitude. Figure 2(a) shows the field (E_0) and frequency (ω_1) dependencies of the magnitude of the harmonic-mixing response, as calculated

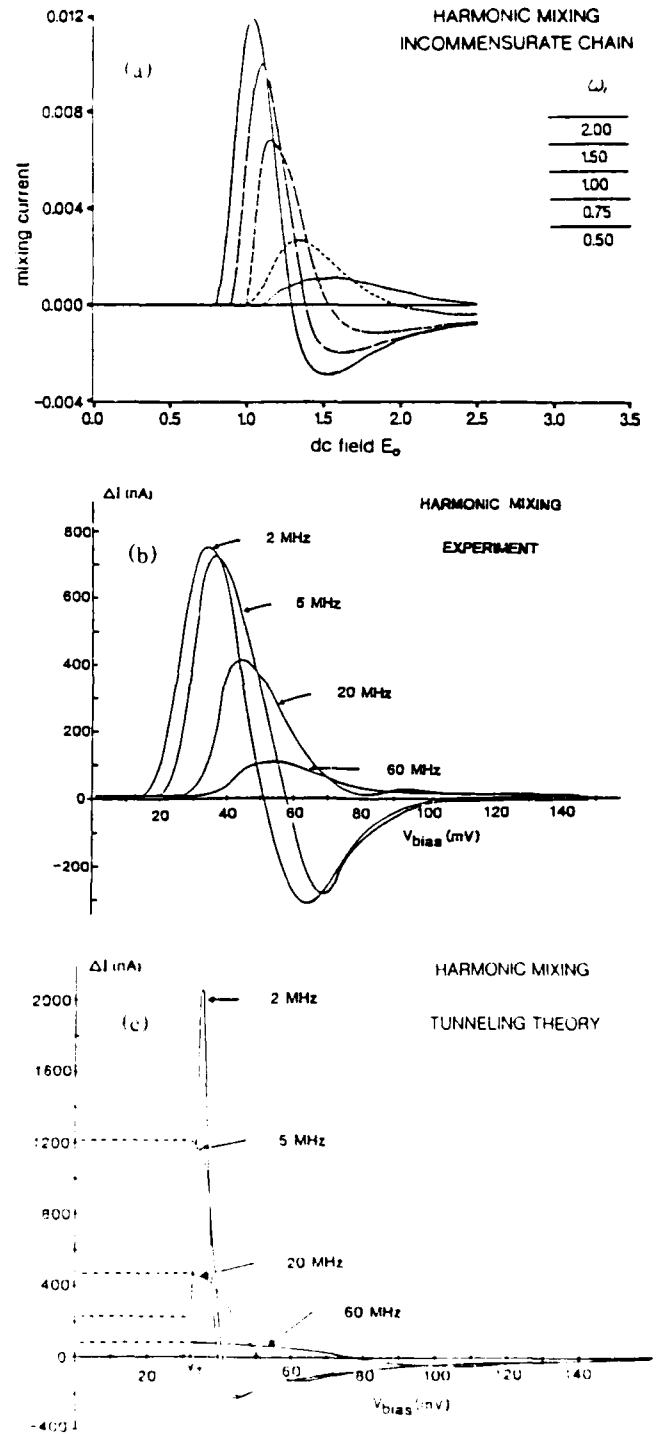


FIG. 2. dc field (E_0) and frequency (ω_1) dependencies of the magnitude of the harmonic-mixing response current ($N^{-1} \sum_j |d_i u_j dt|$). (a) the incommensurate chain, $N = 233$, $P = 3.0$, and $E_1 = E_2 = 0.30$, (b) experiment (Ref. 2), (c) results of a tunneling analysis (Ref. 2).

PUBLICATION 6.
(abstract only)

MODE LOCKING IN CHARGE DENSITY WAVES: A CLASSICAL THEORY

Kenneth A. Cox* and Leigh Sneddon**

*Philip Morris Research Center
PO Box 26583, Richmond VA 23261

**Department of Physics, Brandeis University
Waltham, MA 02254.

ABSTRACT

A substantial disagreement between mode-locking experiments, and predictions based on a classical model, were previously interpreted as proof of the fundamental deficiency of the classical model. We report classical calculations which disprove the predictions, and agree with the experimental data. Contrary to the two previous reports, classical models exhibit complete mode locking at high fields and frequencies. The importance of nonlinear resonance is stressed. We present results for the differential resistance, spectral response and phase boundaries.

IV. Collective Nonlinearity in Solids

When nonlinearity drives many degrees of freedom in dynamic incommensurate systems, these models reproduce the properties of charge density wave conductors (CDW's) in an unexpectedly wide range of experimental situations. The collective and nonlinear properties of these dynamical systems are thus frequently much more important than the precise nature of the pinning potential. In this section, the role of the internal degrees of freedom is elucidated in a variety of experimental observations, for example the existence of the threshold; the shape of the I-V characteristic; ac/dc coupling and interference; dissipative effects; and elastic phenomena.

a) The Threshold.

The fundamental issue of the existence of a threshold in non-commensurate systems can be thought of rather naturally in terms of collectivity. In an incommensurate system, a weak pinning potential excites distortions with the wavevector(s) of the potential, and also their harmonics. The harmonics decay exponentially in strength¹, however, so that an infinite number

¹ S. J. Shenker and L. P. Kadanoff, J. Stat. Phys. 27, 631 (1982)

of degrees of freedom are not excited. There is no threshold².

As the pinning strength is increased, the regime of exponential decay gets pushed out to higher and higher harmonic number (through the nonlinearity). At a finite critical pinning strength, the harmonics never decay exponentially, but only as a power law. At this point all harmonics are contributing and the problem is a collective one. It is precisely at this point that the threshold becomes finite.

A random pinning potential excites all fourier components, no matter how weak it is, because it contains all fourier components. Thus random pinning is a collective phenomenon, no matter how weak the potential. Correspondingly, a random pinning potential has a finite threshold, no matter how weak the potential.

b) The I-V curve.

We can also see collectivity "turn on" in the I-V curve. Consider a straight line, S , through the origin with slope equal to the high field differential conductivity (see Fig 5). The actual I-V curve is offset below S . This "dc offset" can be understood as due to the excitation of a continuum of internal

² Peyrard and S. Aubry, J. Phys C 16, 1593 (1983) and references therein.

degrees of freedom (IDF's). The idea in the above discussion of the threshold works here too. At high fields the potential is effectively weak (since the CDW is moving over it too fast to deform appreciably). The random potential is always collective and produces an offset even at high currents.

The incommensurate potential does not. It can be shown from perturbation theory that the I-V curve approaches the line S at high fields. That is, the offset is not present in low-order perturbation theory. When IDF's are treated to all orders, however, the offset is seen to develop as the field is lowered. This is of course also when the nonlinearity is exciting many IDF's and making the problem truly collective.

c) Interference Effects.

The effect of long range interactions on interference effects provides two slightly more interesting examples of the role of collectivity.

i) "Universality"

First, there is an interesting comparison between the properties of the randomly and incommensurately pinned systems. In the weakly nonlinear regime (weak pinning or high fields) it can be seen from perturbation theory that long range interactions

How can NbSe₃ get around that? By having strong short-range elastic interactions. Short-range elastic interactions favor distortions at long wavelengths. If the dominant distortions are at wavelengths much larger than the CDW wavelength, the washboard frequency will remain relatively well-defined, and the system can behave non-linearly and yet avoid the "catch 22".

Having longer-range interactions, for example Coulomb interactions, however allows shorter wavelength distortions to play a larger role. An infinite-range interaction which is independent of distance, for example, offers a restoring force which is independent of the wavelength of the distortion, and thus does not favor long wavelength distortions at all. The short wavelength distortions will then smear out the microscopic frequency, and the interference features will fall victim to the "non-linear catch 22".

iii) Experimental Results

In a similar fashion to the theory of vortex flow, perturbation theory was used to predict interference features in the frequency-dependent conductivities of sliding CDW's³. Experimental confirmation came immediately in studies of NbSe₃⁴.

³ L. Sneddon Phys. Rev. B29, 725 (1984).

⁴ A. Zettl and G. Gruner Phys. Rev. B29, 755 (1984).

wash out the ac/dc interference features of randomly pinned systems (see below). In the same regime, however, perturbation theory shows that an incommensurate chain will produce ac/dc interference features whether the elastic interactions are short-or long-range.

What happens to incommensurate chains in the strongly non-linear sliding regime, where the interference features are strong? The features become vulnerable to long range interactions (see Publication 1). Thus again, as we approach threshold in FK systems we enter a collective regime in which their properties imitate those of randomly pinned systems.

ii) "Non-linear Catch 22"

Why do long range interactions wash out interference features in randomly pinned systems? The answer is that the interference is subject to a "nonlinear catch 22". Interference is of course a nonlinear effect, and the source of nonlinearity is the pinning, so for interference to exist the system must be being distorted by the pinning potential. This distortion, however, locally and incoherently modulates the CDW wavelength, and hence smears the washboard frequency. Thus, to get ac/dc coupling at all, the system must suffer a smearing out of the frequency that defines the interference feature.

The experimental results showed what were called inductive dips: the dielectric constant can become strongly negative at the interference feature. The non-perturbative solution of the incommensurate chain then showed us (Publication 1) that these inertial dips, as well, could be understood as the nonlinear, collective response of a classical, massless system.

TaS₃, however, did not show these features⁴, and the suggestion was made that long-range Coulomb interactions in the semiconducting TaS₃ were responsible (Publication 1). The mechanism may be precisely the non-linear catch 22 outlined above. This proposal can be probed a little further, however. Coulomb potentials will be easier for the conduction electrons to screen away if the underlying charge fluctuations occur at low frequencies; and also if the normal conductivity is high. Mihaly et al⁵ examined both the frequency- and temperature-dependence of the interference properties of TaS₃. They found that sharp features did indeed re-emerge at lower applied frequencies and also at higher temperatures, where the normal conductivity is enhanced in the semiconductor. While careful qualitative tests still remain to be performed, these results are clearly qualitatively in agreement with the "catch 22".

⁵ Mihaly et al

d) Viscosity Enhancement

Collectivity also has dissipative consequences. Because a CDW carries condensed charge, whenever it is deformed there will be, as noted above, charge accumulation, which the normal carriers will then strive to screen. Normal currents are dissipative, however, and these normal screening currents were predicted⁶ to enhance the viscosity or damping of the CDW motion, the effect predicted to grow larger as the temperature is decreased, roughly proportionally to the normal resistivity in the semiconducting materials. The predicted effect on the temperature-dependence of the I-V characteristics was first qualitatively verified by Monceau. About two years after the theoretical prediction, another series of experiments by Fleming et al. also confirmed that the viscosity had essentially the same temperature-dependence as the normal resistivity.

e) Elastic Phenomena

The collective nature of CDW transport also plays an important role in the elastic properties of CDW conductors. A rigid CDW can couple to the lattice modes⁷, enabling a sliding CDW to make the sound velocity anisotropic. The effect would be

⁶ L. Sneddon Phys. Rev. B29, 725.

⁷ S. N. Coppersmith and C.M. Varma Phys. Rev. B30, 3566 (1984).

very small, and an analytic function of the CDW current. When the internal degrees of freedom of the CDW are taken into account, however, the effect becomes much larger (see Publication 3). Mathematically, the effect becomes first order in the lattice-CDW coupling, while without the IDF's, only second order effects are possible. Physically, the IDF's are enabling the CDW to get a "grip" on the lattice, so that to deform the lattice, one must also deform the CDW, and this contributes to the lattice stiffness. As the CDW starts to move relative to the lattice, it has less time to for the IDF's to adjust, and the grip of the CDW on the lattice is not as strong, and the stiffness of the lattice diminishes, as seen experimentally. Further, the IDF's produce a sliding threshold at which the dynamics is singular. This is consistent with the experimental observation⁸ of a fractional exponent in the Young's Modulus.

The collective nature of the CDW transport also plays an important role in the internal friction of elastic vibrations. Below threshold, many of the IDF's are pinned by the pinning potential and their response to an external driving is limited. It is likely that there is a gap in their excitation spectrum. As the applied electric field passes above threshold, the gap would vanish, and the IDF's suddenly become more easily excited. The excitation of IDF's dissipates energy, and thus leads to a marked increase in the internal friction.

⁸ J.W. Brill and W. Roark, Phys Rev. Lett. 53, 846 (1984).

f) Conclusion

If the function of randomness is only to introduce collectivity and nonlinearity, then we have a rather satisfactory situation. At high fields, incommensurate systems are not collective, and so randomness is essential. At high fields, however, we can use perturbation theory to solve random pinning. At low fields, incommensurate systems become collective as well as nonlinear and thus much more realistic. Further, it has proved possible to solve for many of their properties in this regime. Thus incommensurate systems may well be, when combined with the HIGH-field solutions of randomly pinned systems, completing a solution of sliding CDW's by providing a theory which includes the most important physical features, and yet which is also soluble, in the LOW-field, or strong coupling, sliding regime.

V. The Threshold: a Surviving Challenge

When the threshold field for conduction is approached, the incommensurate chain becomes strongly distorted at all length scales. As a result, the threshold combines the all the richness of critical phenomena (such as singular responses with universal exponents) with the additional challenge of being a dynamic process, far from equilibrium.

The ideas of the renormalization group have been used

successfully to construct a transformation which has a fixed point describing the depinning transition in incommensurate dynamics⁹. This transformation establishes the full universality class of this transition. The work is particularly novel and will, it is hoped, provide a basis for a theory of the threshold of CDW dynamics. This extension, to the asymmetric, dynamic case of the conduction threshold, is the subject of ongoing work.

⁹ L. Sneddon, A.J. Kassman, S. Liu manuscript in preparation.

END

DATE

FILM

JAN
1988